Photopolymerization in 3D printing of tissue-engineered constructs for regenerative medicine

Alla N. Generalova,[a, b] **Polina A. Demina,**[a, b] **Roman A. Akasov,**[a, b] **Evgeny V. Khaydukov** [a, b]

*[a] Shemyakin–Ovchinnikov Institute of Bioorganic Chemistry, Russian Academy of Sciences,
ul. Miklukho-Maklaya 16/10, 117997 Moscow, Russian Federation*
*[b] Federal Scientific Research Center 'Crystallography and Photonics', Russian Academy of Sciences,
Leninsky prosp. 59, 119333 Moscow, Russian Federation*

The progress in the field of tissue engineering is largely driven by the development of 3D laser printing technologies, which allow precise creation of hydrogel scaffolds containing cells (the so-called tissue-engineered constructs), using photoinduced radical reactions of polymerization and crosslinking. The review considers the main mechanisms and features of such reactions, presents the most common materials for photocompositions, including natural and synthetic polymers and precursors, and describes various mechanisms for photoinitiator activation. Advances in the field of photopolymerization enable application of modern laser 3D printing techniques based on extrusion and stereolithography to design tissue-engineered constructs in a wide range of sizes and shapes with a finely organized architecture. The integration of such methods with the methods of bioengineering and cell technology is discussed, including for the creation of tissue-specific and *in vivo* polymerized constructs.
The bibliography includes 225 references.

Contents

1. Introduction

Tissue engineering currently stands out among innovative technologies, aimed at solving the problem of organ and tissue donor shortages for transplantation to patients with irreversible injuries. Tissue engineering is based on inter-disciplinary technologies that allow construction and grow-ing biofunctional materials both inside and outside the patient body in order to replace or regenerate damaged tissues or organs. This approach implies formation of a three-dimensional tissue structure with the required phys-ico-chemical properties, including the mechanical ones, in place of a defect. Besides, this process is accompanied by restoration of biological functions of the damaged organ, which is the main difference from application of traditional implants made of inert materials.[1]

The most promising field in tissue engineering is based on the creation of tissue-engineered constructs (TECs) representing the integration of three components: polymeric materials in the form of matrix-carriers, the so-called scaf-folds, living cells, and biologically active molecules. A tissue-engineered construct provides conditions that mimic the environment in the replaced tissues of the body, which determines penetration, colonization, attachment and pro-liferation of either allogeneic or autologous cells of the patient. Such an environment should reproduce the main characteristics of the native extracellular matrix at the cellular and subcellular level as closely as possible and facilitate the synthesis of new tissue.[2] Scaffolds play an

2 of 26

A.N.Generalova, P.A.Demina, R.A.Akasov, E.V.Khaydukov
Russ. Chem. Rev., 2023, **92** (2) RCR5068

important role in stimulating tissue regeneration providing the necessary physical, chemical, mechanical and biological properties, including biocompatibility, biodegradation, porosity, mechanical strength, elasticity. Moreover, their surface should have high adhesion to cells in the absence of cytotoxicity, immunogenicity, and pyrogenicity.[3, 4] The properties of scaffolds are primarily determined by the nature and chemical composition of the source material. The most widely used materials are natural and synthetic polymers that allow the formation of scaffolds with a variety of properties. In particular, it is possible to obtain polymer-based hydrogels, which have recently become of great interest for their application as scaffolds. This is because the structural and biochemical properties of such hydrogels are similar to the properties of extracellular matrix of most tissues, and their mechanical properties can be adapted to the properties of soft tissues.[5] The hydrophilic properties of hydrogels promote cell adhesion, and the porous three-dimensional structure facilitates the diffusion of cells and nutrients.[6] The hydrogel production is based on the crosslinking reaction of hydrophilic monomers, oligomers or macromonomers, which determines its structure, shape, size and degradation rate. The crosslinking process can occur both by covalent bond formation (radical or cationic polymerization, reactions of addition, condensation or enzyme catalysis, reactions induced by gamma rays or electron beams, *etc.*), and by non-covalent interactions based on the action of electrostatic or hydrophobic forces, Van der Waals forces, solvation, *etc.*[7] However, when forming hydrogels, there is a problem of controlling their internal architecture (*e.g.*, porosity, pore size, their spatial arrangement and relationships) and distribution of the composition components within the hydrogel volume. In addition, it is almost impossible to include living cells and signal molecules at the stage of hydrogel formation due to the use of solvents incompatible with cells, long time or harsh conditions of gel forming reaction.[8, 9]

One of the methods that eliminates these drawbacks is the light-driven covalent crosslinking. This can be a photopolymerization reaction if hydrogels are formed from monomers (oligomers), or photoinduced crosslinking involving macromonomers (*e.g.*, biomolecules).[†] As compared to the above methods,[10] photopolymerization proceeds rather quickly (from a few milliseconds to minutes) at

---

† In this review, to simplify presentation, the term 'photopolymerization' will be used in both cases.

low doses of initiating radicals and does not require high temperature or extreme pH values.[11] The process can be implemented in the presence of cells and bioactive molecules, and without deposition of cells in the initial reaction solution, which is called a photopolymerizable composition (photocomposition). As a rule, the light-driven chemical reactions are very efficient that is associated with the formation of a minimum amount of byproducts. This is an important condition for the production of biocompatible scaffolds containing living cells.

In recent years, significant efforts of researchers have been focused on the creation of photocompositions required for the formation of three-dimensional (3D) functional scaffolds, which are called ink, from monomers (oligomers or macromonomers) with good biocompatibility, bioactivity and degradability.[12] Note that light allows non-contact spatial and temporal control of the degree of macromolecule crosslinking, which determines the ability to make 3D objects of different shapes that can be integrated into the structure of native tissue.

The greatest success in the field of TEC fabrication by photopolymerization was achieved by using additive technologies, namely 3D photoprinting, to produce copies of three-dimensional computer models of products and prototypes, based on their step-by-step formation (in the form of layers) when adding material to the substrate.[13, 14] This technology is based on two main approaches:

— photoprinting based on extrusion, when the crosslinking reaction proceeds under the action of light as the ink is supplied or deposited from the extrusion device;

— photoprinting based on lithography, which involves the light-driven transition of the ink to a solid state.

The issue of obtaining 3D models in the process of photopolymerization using 3D printing is covered in the literature in sufficient detail (*e.g.*, see reviews[2, 12, 15–17]). However, there is no systematized information on the action of photoinitiators and the mechanism of the main photoreactions occurring during the transformation of ink into crosslinked hydrogels (scaffolds) under the action of light. Usually such studies are limited to photoreactions activated by UV and visible radiation and do not affect the IR spectrum.

This review presents traditional and recently developed reactions, as well as their mechanisms and peculiarities of implementation, used to form the 3D structures when irradiated with light of a wide spectrum — from ultraviolet to infrared one. Such reactions include chain free-radical

A.N.Generalova. Professor**,** Doctor of Chemical Sciences, Chief Researcher, Head of the Laboratory of Polymers for Biology, IBKH RAS; Senior Researcher, Laboratory of Laser Biomedicine, FSRC 'Crystallography and Photonics' RAS.
E-mail: angeneralova@gmail.com
Research interests: synthetic and natural high-molecular compounds, including their modification of surfaces of inorganic luminescent nanoparticles to solve the problems of bioimaging, diagnosis and therapy of pathologically altered tissues; nanobiotechnology, including obtaining polymeric structures in the process of reactions photoinduced by IR light using anti-Stokes nano-phosphors.
P.A.Demina. Junior Researcher, Laboratory of Laser Biomedicine, FSRC 'Crystallography and Photonics' RAS; Junior Researcher Laboratory of Polymers for Biology, IBKH RAS.
E-mail: polidemina1207@yandex.ru
Research interests: upconversion nanoparticles, functionalization of surfaces with biopolymers for *in vitro* and *in vivo* studies, preparation of scaffolds by IR-induced 3D photopolymerization.

R.A.Akasov. PhD, Senior Researcher, Laboratory of Laser Biomedicine, FSRC 'Crystallography and Photonics' RAS; Researcher, Laboratory of Biomedical Materials, IBKH RAS.
E-mail: roman.akasov@gmail.com
Research interests: experimental biological models for *in vitro* and *in vivo* studies, cell technologies: 3D cultures, nanosystems and their application in biomedicine; methods of laboratory diagnostics and therapy, and *in vivo* scaffold implantation.
E.V.Khaydukov. Professor**,** Doctor of Physical and Mathematical Sciences, Senior Researcher, Laboratory of Polymers for Biology, IBKH RAS; Head of the Laboratory of Laser Biomedicine, FSRC 'Crystallography and Photonics' RAS.
E-mail: khaydukov@mail.ru
Research interests: development of upconversion nanoparticles for biomedical applications, in particular, in biosensorics, bioimaging, early detection of tumor diseases, and phototherapy; optical coherence tomography; photochemistry of riboflavin, upconversion processes.

Translation: S.B.Karlova

A.N.Generalova, P.A.Demina, R.A.Akasov, E.V.Khaydukov
Russ. Chem. Rev., 2023, **92** (2) RCR5068

3 of 26

polymerization, thiol-ene polycondensation, redox radical polymerization, and controlled radical polymerization. The most common ink materials and types of initiating systems necessary for photopolymerization and fabricating scaffolds of the required architecture are considered. The approaches to produce scaffolds in a wide range of sizes, various shapes with finely organized structure and surface morphology by using modern laser technologies of 3D printing based on extrusion and stereolithography are demonstrated. The methods for scaffold creation *in vitro* and their implantation are shown with an emphasis on the high-potential methods of scaffold formation directly in the damaged area (*in situ*), which ensures a high accuracy of tissue reconstruction. The presented approaches allow the creation of structured TECs with cell cultures both in the process of synthesis and when cells are incorporated into the final products for wide utilization in biomedical research.

2. Basic photoinduced reactions in 3D printing

Three components are necessary to obtain TECs in the process of 3D photopolymerization: light, photopolymerizable composition (ink), and cells. The most promising are inks, whose irradiation with light leads to formation of hydrogels. Hydrogel structures of liquid ink in the process of 3D photopolymerization are traditionally obtained under the action of UV and visible radiation using radical initiating systems. The latter activate chain reactions and participate in double bond hydrotiolation, redox and controlled reactions by the mechanism of 'live' chains, as well as in the presence of cationic initiation systems. However, the use of cationic systems, despite the possibility of reaction proceeding by the mechanism of living chains, which provides high substrate conversion, is not suitable for working with living systems. This is because cationic initiators generate strong acids that negatively affect cell cultures.[18] In addition, the presence of water slows down or even completely inhibits the cationic polymerization reaction.[19] In addition, the living chains mechanism can be implemented only in the absence of oxygen, making impossible the creation of scaffolds with cell cultures. For this reason, cationic systems will not be considered in this review.

Of particular interest is photopolymerization under the action of near IR (NIR) light, which affects tissues by low-energy light quanta at great depths and provides a safe environment for cell life in 3D technologies.[20] For this purpose, initiation systems for two-photon polymerization and systems based on energy transfer from the donor, excited by NIR light, to the acceptor, which can generate radicals that enter into the polymerization reaction, are being developed.[15]

2.1. Free radical chain reaction
Typically, the ink composition includes a radical-reactive monomer (oligomer, macromonomer), an initiator or initiating system, and various additives such as drugs, porogens, mechanical strength regulators, *etc.*[15] Acrylate and methacrylate monomers and oligomers are most widely used in 3D photopolymerization by the chain free-radical mechanism in the TEC production. Free-radical initiators, described in Section 3.2, are used to activate these monomers.

In photoinduced chain polymerization of ink by the radical mechanism, three stages can be distinguished: initiation, chain growth and chain growth termination
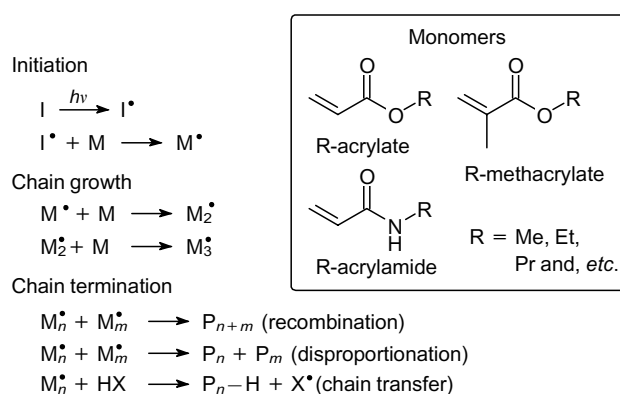

Figure 1. Scheme of radical chain polymerization and examples of basic monomers. The following designations are used: I is initiator, M is monomer, P is polymer, R is alkyl group.

(Fig. 1). Each stage has its own kinetic features, which can affect the micro- and macrocharacteristics of the resulting hydrogels.

The polymerization process begins with generation of radicals under the action of light with participation of a photoinitiator or a photoinitiator system, which form radicals that can activate the monomer (oligomer) due to photolysis or electron (hydrogen atom) attachment. The rate of radical formation from the initiator depends on the incident light intensity, the photoinitiator activity and concentration, the quantum yield and the number of effective radicals generated per one act of photolysis. Then these free radicals react with vinyl groups of monomers (oligomers) to form new covalent bonds and reactive radicals. The radicals enter into subsequent reactions with vinyl groups, which leads to the growth of a polymer chain. The growth process ends when the monomer (oligomer) is exhausted and due to reactions of chain growth termination such as recombination of radicals, disproportionation of radicals with formation of saturated and unsaturated end groups, transfer reaction from the growing chain to other components of the reaction medium — solvent, monomer, *etc.*[12]

Examples of basic monomers with a vinyl end group capable of entering into light-driven chain radical polymerization are shown in Fig. 1. The most common inks for making 3D objects are (meth)acrylate monomers (oligomers): polyethylene glycol diacrylate, triethylene glycol dimethacrylate, copolymer of bisphenol A with glycidyl methacrylate, trimethylolpropane triacrylate, bisphenol A ethoxylate diacrylate.[15]

The structure and density of crosslinking of the polymer chains, formed by radical chain polymerization can be controlled by changing the concentration of initiator, the number of vinyl groups (*e.g.*, by varying the monomer or oligomer concentration) and the light intensity. As a rule, mechanically strong scaffolds with long degradation times in the case of biodegradable materials are formed at a high degree of crosslinking.[9] However, the different lengths of the growing kinetic chain determine heterogeneity of the scaffold structure. This heterogeneity is associated with the concentration gradient and diffusion limitations, since the high rate of kinetic chain formation leads to auto-accelerated chain growth and diffusion-controlled chain termination. In particular, steric hindrances that arise in the process

of polymer network formation limit chain termination reactions, and, correspondingly, the total concentration of radicals increases. The rate of polymerization increases and the auto-acceleration process starts, leading to formation of a heterogeneous system in which intramolecular chain transfer reactions can also take place. As a result, the radicals responsible for branched and cyclic structures can be formed along the chain,[21] *i.e.* the heterogeneity of the scaffold structure increases.

The chain nature of polymerization determines the high rate of hydrogel formation, but the dependence of kinetics on many factors causes a number of limitations. First of all, we should note the inhibitory effect of atmospheric oxygen, required for TEC formation with cells. The negative effect of oxygen on polymerization is manifested in deactivation of the excited states of the initiator and formation of inactive peroxide radicals, which affects the efficiency of the entire process. This leads to incomplete crosslinking of the material during 3D photopolymerization and reduces printing accuracy, and also has an effect on the shape retention over time,[22] which is crucial for complex structure creation. In addition, it is necessary to use low intensity radiation and minimize the number of generated radicals, since both of these factors have a cytotoxic effect on cells.[23]

The above limitations of photoinduced free-radical chain reactions (relatively poor control of crosslinking kinetics, inhibitory effect of oxygen, presence of unreacted double bonds, formation of heterogeneous structures) necessitates the development of new approaches to scaffold production. One of the ways is the use of orthogonal click reactions for photoinduced radical crosslinking.

2.2. Radical polycondensation based on thiol-ene addition

Orthogonal click reactions based on hydrotiolation of double bonds (thiol-ene reactions) have attracted much attention due to more precise control of light-driven radical crosslinking as compared to the chain processes. Thiol reactions with highly reactive carbon–carbon double bonds are well known.[24] They can proceed as polycondensation (radical step polymerization), which will be discussed below, or by the reaction of Michael addition.[25] Thiol reactions provide polymer scaffolds with less heterogeneity because they allow control over crosslink density, cell size and mechanical properties by varying functionality, length and concentration of a crosslinking agent. In addition, thiol-ene reactions are insensitive to the presence of water and oxygen and can proceed under mild conditions with higher efficiency, selectivity and rate as compared to the chain radical process.[26]

Under the action of radicals formed at the stage of initiation, the sulfide groups of thiol-containing molecules are converted into reactive thiyl radicals (Fig. 2). Then, these intermediate thiyl radicals form thioether bonds with molecules containing vinyl groups. The growth of a polymer chain occurs according to a stepwise mechanism, in which the sequential addition of monomers (oligomers, macro-monomers) leads to a gradual increase in molecular weight. When using multifunctional crosslinking agents, a network structure is formed. To obtain scaffolds, a reactive oligomer and a multifunctional thiolated crosslinking agent are usually utilized. As in the case of a chain reaction, the rate of polycondensation and the properties of a final product, depend significantly on a number of factors. In general, the thiol-ene reaction proceeds very quickly (within a few seconds) with crosslink formation and this allows the
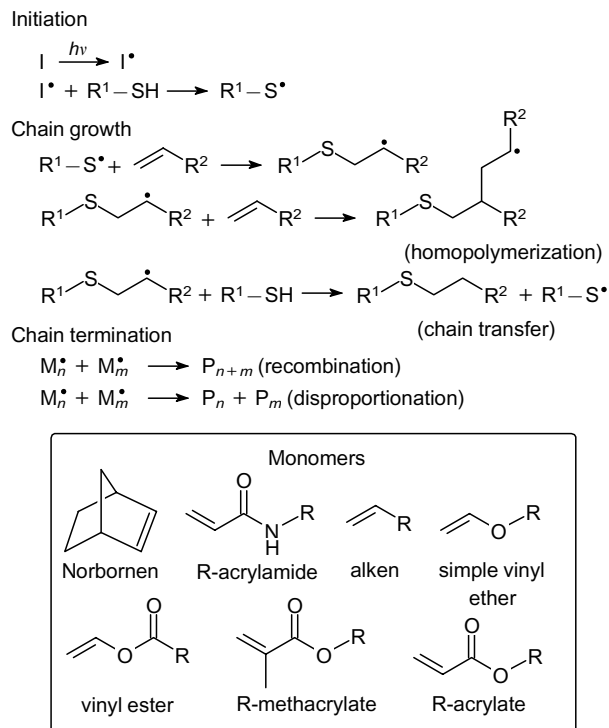

Figure 2. Scheme of thiol-ene addition.

control of the final product properties by controlling the crosslinking degree.[15]

The main vinyl monomers capable of participating in the thiol-ene reaction are shown in Fig 2. The following thiol-containing compounds are most widely used as the second component for obtaining 3D objects: tris(3-mercaptopropionate) trimethylolpropane (TMPMP), tetrakis(3-mercaptopropionate) pentaerythritol (PETMP), tris[2-(3-mercaptopropionyloxy)ethyl]isocyanurate (TMI) and tetrakis(2-mercaptobutanoate) pentaerythritol (PE-1).[15]

It is worth noting that some vinyl derivatives, along with the thiol-ene reaction, can simultaneously participate in free radical chain processes that result in scaffold formation by two mechanisms. This case can be considered as mixed polymerization. For example, (meth)acrylates form crosslinks with multifunctional thiols during polycondensation and also enter into a radical chain reaction, *i.e.* copolymerization can take place in one material. This format of photoinduced crosslinking allows expansion of scaffold properties during their production. However, the complex kinetics of these radical processes can potentially cause phase separation in the scaffold formed by different mechanisms.[27]

The reactivity of vinyl groups is determined by their electron density, stability of intermediate radicals, and steric hindrances. End groups with high electron density react more actively than groups in the main chain or groups with lower electron density. The conversion of monomers (oligomers, macromonomers) depends not so much on the kinetics of various thiol-ene reactions but on the vinyl group ability to polymerize in a given material and such effects as auto-acceleration and diffusion-controlled chain termination determined by the crosslinking degree. These factors allow one to reach the same substrate conversion for processes with different kinetics. In addition, thiol-ene

A.N.Generalova, P.A.Demina, R.A.Akasov, E.V.Khaydukov
Russ. Chem. Rev., 2023, **92** (2) RCR5068

5 of 26

reactions provide more precise control over the depletion of vinyl groups compared to the chain process since the crosslinking degree is controlled by the concentration of the crosslinking agent rather than the reactive groups. This allows consistent, controlled crosslinking, as well as incorporation of biomolecules important for tissue engineering into the scaffold network.[28]

However, there are a number of restrictions for the wide application of thiol-ene systems in 3D photopolymerization. The scaffolds obtained in this way are characterized by a short shelf life and an unpleasant odor, caused by formation of byproducts with a disulfide bond, which can be easily oxidized. Moreover, thiol-ene reactions, due to the stepwise growth kinetics, lead to formation of homogeneous hydrogel networks with flexible thioether bonds. As a result, soft materials with a low elasticity modulus are obtained.[29] Though, the mechanical properties of the resulting products can be improved by introducing a second monomer, such as methacrylate,[15] or an oligomer, such as oligourethane with norbornene end groups.[30] The storage stability of the source thiols can be improved by using stabilizers, preventing formation of disulfides,[31] or by creating new monomers. For instance, Chen *et al.*[32] have synthesized a highly stable double thiol-ene photocurable composition containing *tetrakis*(3-mercaptobutanoate) pentaerythritol (PE-1) and triallyl-1,3,5-triazine-2,4,6(1*H*,3*H*,5*H*)-trione (TTT), which showed high thermal stability during storage.

In general, the thiol-ene photocrosslinking reaction is a very promising approach to produce scaffolds with finely tuned properties by 3D photopolymerization.

2.3. Redox radical reactions

Redox reactions are also used to produce scaffolds in the course of photopolymerization. These reactions can involve both monomers (oligomers) with vinyl groups, conventional for radical chain polymerization (see Fig. 1),[33, 34] and polymers containing groups, which can be activated during redox reactions under the action of photosensitizers and then participate in radical polymerization or crosslinking reactions.[35]

Dyes or additives, effectively absorbing light and passing into excited states, can be used as photosensitizers, capable of oxidizing (reducing) reactive groups. Photosensitizers absorb light of longer wavelengths and they do it with greater efficiency than organic small molecules. The energy of the absorbed photon can be converted into a chemical potential that affects organic substrates in various ways.[36] The photosensitizer must have a high absorption coefficient at the wavelength of the exciting light, a high quantum yield, and a sufficient stability to catalyze the photoreaction.[37] To generate radicals, it is necessary to use an initiating system of type II (see Section 3.2.2) that contains a photosensitizer and a co-initiator. In this case, the excited photosensitizer molecule reacts with the corresponding co-initiator, which exhibits the properties of an electron donor or acceptor or hydrogen atom donor responsible for generation of corresponding radicals or radical ions.[38] The fulfillment of these conditions determines the ability of photosensitizers to generate free radicals through electron transfer or hydrogen atom abstraction from the substrate (Fig. 3). Further polymerization proceeds according to the scheme of the radical process, in which the stages of chain growth and chain termination are distinguished (see Fig. 1). The ink composition includes traditional radical monomers (oligomers, poly-
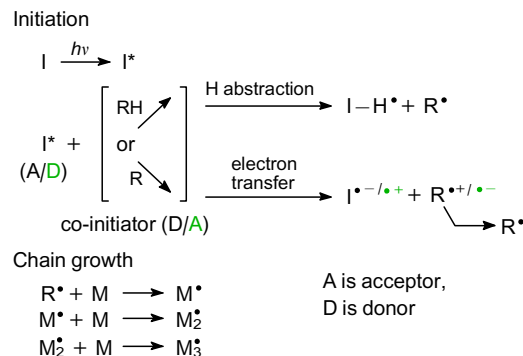

Figure 3. Scheme of redox radical photopolymerization (chain termination reactions see in Fig. 1).

mers) containing vinyl groups, as well as, for example, moieties of tyramine or tyrosine.[12]

It is important to note that, in the presence of oxygen, photosensitizers additionally undergo side reactions, which lead to the formation of singlet oxygen, superoxides, and then hydrogen peroxide.[37] These side reactions cause regeneration of the ground electronic state of photosensitizers and consumption of the formed radicals. As a result, the rate of photoreactions increases as well as the degree of reactive group crosslinking.

Side reactions of the first type include energy transfer from a photosensitizer in an excited (triplet) state to an oxygen molecule in the ground state. As a result, singlet oxygen, which can easily oxidize hydroxyl, sulfide, and amino groups, is generated. After reactions associated with electron transfer and hydrogen atom abstraction from the substrate, the photosensitizer radicals can enter into secondary reactions with triplet oxygen, accompanied by superoxide formation. In addition, primary radicals can interact with each other and react with oxygen in the ground state, resulting in formation of hydrogen peroxide.

It is known that the reaction of photoinduced crosslinking hardly proceeds under the anaerobic conditions.[35] Reactive oxygen species in the form of radicals may not participate in the process of radical crosslinking of monomers (oligomers, macromonomers), but they are necessary for activation of the photosensitizer and generation of reactive radicals by the initiating system. Therefore, a very important property of photosensitizers is the ability of easy energy transfer to triplet oxygen. This feature of redox polymerization determines the significant difference from the radical chain process, when oxygen inhibits the photoinduced crosslinking reaction. Examples of initiating systems are presented in Section 3.2.2.

When using photosensitizers in the process of 3D photopolymerization, it is necessary to take into account their cytotoxic properties, as well as the ability to generate reactive oxygen species upon irradiation. These side effects can be minimized by reducing the concentration of photosensitizers to a level that allows maintaining the kinetics of the photocrosslinking reaction without a significant cytotoxic effect on cells.

2.4. Controlled radical polymerization

Controlled radical polymerization (CRP) is often used to synthesize polymers with specific compositions, topologies, and architectures. It is based on the replacement of irreversible bimolecular chain termination with a reversible reac-

tion of radical growth under the action of agents that transfer the chains into an inactive state. As a result, macromolecular radicals participate in successive activation—desactivation cycles. Activation at the end of the polymer chain leads to the appearance of a labile end group capable of cleavage under certain conditions to form a radical that can continue the growth of the polymer chain. The process of repeated cycles of radical activation—desactivation ensures the stepwise growth of all chains during polymerization.[39]

In particular, the CRP methods are being developed that use light to detach the end group, which transfers into a growing radical, and this allows spatiotemporal control over the process of chain growth.[40, 41] Currently, active application of such CRP methods for scaffold production by 3D photopolymerization starts.

2.4.1. Controlled radical polymerization with addition—fragmentation chain transfer

Acrylate-based monomers (oligomers) are most widely used as a starting material for 3D photopolymerization resulting in a rigid hydrogel network due to the high rate of polymer chain growth. However, the lack of control over this reaction leads to formation of inhomogeneous materials with uncontrolled chain crosslinking and, accordingly, brittle materials, which significantly narrows the scope of their application. The key direction in the development of 3D photopolymerization is the creation of new ink that forms homogeneous networks in the process of radical stepwise growth similar to the thiol-ene reaction, but devoid of its drawbacks (see Section 2.2).[42] Such ink is suitable for fabrication of 3D structures with high impact toughness and low shrinkage stress.[43]

One of the approaches is based on radical polymerization with the addition—fragmentation chain transfer (AFCT). During this polymerization, the growing radical is attached to the AFCT agent, followed by deactivation (fragmentation) of the resulting adduct radical, which leads to the formation of a polymer chain with a vinyl end group and a radical capable of initiating a new chain (Fig. 4).[44] This method allows the control of the polymer molecular weight and introduction of functional end groups. The process is very similar to the reversible addition—fragmentation transfer polymerization (RAFT),[45] but the growing radical reacts with the AFCT agent much slower than in a controlled living RAFT system (see Fig. 4).[44]

Chain transfer agents in the AFCT process, such as allyl sulfides,[46] allylsulfones,[42] vinyl sulfone esters,[42] are the promising additives for photopolymerizable ink controlling the formation of a uniform network, which improves the thermal and mechanical properties of the material.

However, the use of AFCT polymerization reduces the rate of radical reaction, especially at high concentrations of agents. This can increase significantly the time required for layer photocuring and, accordingly, duration of 3D printing based on the creation of multilayer structures.

2.4.2. Living controlled radical polymerization with the addition—fragmentation chain transfer

In the RAFT-polymerization, free-radical polymerization can be implemented using the mechanism of living chains, in which re-initiation, introduction of new monomers into the formed polymer network and visible- or UV-light-induced functionalization are possible.[47] This polymerization proceeds with the help of agents containing groups with an unsaturated bond at the end of the chain (mainly C=S), such as dithioether, dithiocarbonate, dithiocarbamate, etc., which enter into the exchange reaction due to addition and fragmentation.

To date, only a few examples of RAFT agent utilization for 3D photopolymerization are presented in the literature. In particular, hydrogels based on acrylates and acrylamides, such as *N*-isopropylacrylamide, n-butyl acrylate, and poly-ethylene glycol methyl ester acrylate, can be obtained by the mechanism of light-driven living radical polymerization in the presence of sodium trithiocarbonate derivatives as a RAFT agent and 10-phenylphenothiazine as an organic photochemical redox initiator. Using this system, we can effectively switch the state of radicals in the growing chain from addition to fragmentation and back under the action of visible and UV light. During the polymerization, the molecular weight of polymers increases linearly without a gel effect. The proposed mechanism of this process is shown in Fig. 4. The electron transfer from the photoexcited photocatalyst (I*) activates the molecule of sodium trithiocarbonate with the formation of $P_n^{\bullet}$ radical, which participates either in the growth reaction or in chain transfer by the RAFT mechanism. Sodium trithiocarbonate (TTC radical in the case of UV light; TTC anion and an ionic complex with $I^{+\bullet}$ in the case of visible light) can deactivate the growing polymer chain to form a polymer containing a TTC fragment at the end of the chain, and the photoinitiator in the ground state. Under the action of light these components are able to re-enter the catalytic cycle (reversible activation).

Photocatalyzed RAFT polymerization enables embedding of a new monomer into the product by the mechanism of living chains. Depending on the nature of monomers and the number of crosslinks, secondary gels with a different network structure and, accordingly, with different chemical and mechanical properties can be obtained on the basis of the initial gel.[48] However, the rate of CRP by the mecha-
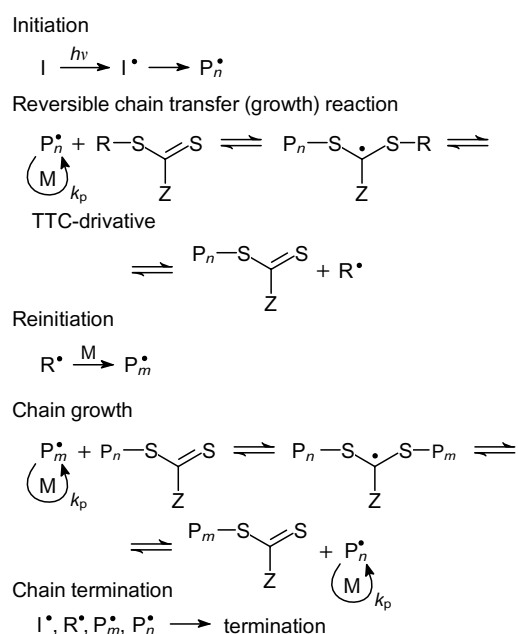

Figure 4. Scheme of living controlled radical polymerization with addition-fragmentation chain transfer (RAFT). TTC is trithiocarbonate, Z is activating group.

A.N.Generalova, P.A.Demina, R.A.Akasov, E.V.Khaydukov
Russ. Chem. Rev., 2023, **92** (2) RCR5068

7 of 26

nism of living chains is lower than that of radical chain polymerization, which may limit its use in 3D photopolymerization if it is necessary to assemble the product rapidly.

3. Main components of photocompositions

The necessary components of photopolymerizable compositions (ink) are as follows: a material, which can form hydrogel structures; a photoinitiating system that generates radicals under the action of UV, visible or IR radiation, and cells that can be included in the structure both at the stage of ink photopolymerization and after the sample preparation. The formation of TECs in the form of scaffolds with cells and their application in biomedical research are discussed in Section 5. Components that improve rheological and mechanical properties, as well as porosity, degradation, visualization of hydrogels, *etc*., can be introduced into the photocomposition.

3.1. Ink composing materials
Scaffolds in the form of hydrogels are water-swollen polymer networks, consisting of natural and (or) synthetic materials, usually biodegradable. Great prospects for the use of hydrogels in tissue engineering are associated with the possibility of their rational design to mimic the functions and structures of damaged or lost tissues. The highly hydrated environment of hydrogels reproduces the aqueous environment of tissues and allows the introduction of cells, bioactive molecules and drugs into them.

In addition, the physicochemical properties of hydrogels can be easily adjusted for specific tasks. For example, by adjusting the crosslinking degree, we can obtain gels with well-defined network parameters, which allow the diffusion of components to ensure the supply of nutrients or oxygen to the cells. Controlling the crosslink density, which also affects the mechanical properties of hydrogels, enables the formation of hydrogel networks whose viscoelastic properties and stiffness are comparable to those of native tissues. An important property of hydrogels is the possibility of their biofunctionalization, for example, with bioactive molecules, various labels or drugs to improve adhesion, migration, visualization, proliferation and differentiation of encapsulated cells.[49]

The unique properties of hydrogels listed above determine the prospects of their application as scaffolds for repair of affected tissues. Materials on the basis of which hydrogels can be obtained in 3D photopolymerization are classified according to their origin: natural, synthetic and hybrid ones. Examples of such materials are presented below.

3.1.1. Natural polymers
Natural compounds are widely used as the main component of ink, since they are usually characterized by high biocompatibility, biodegradability and bioactivity. One of these compounds is gelatin, which is formed during collagen denaturation. Gelatin contains adhesive peptide sequences (*e.g*., RGD peptide) that allow embedded cells to attach and proliferate in gelatin hydrogels. In addition, gelatin contains peptide sequences, sensitive to endogenous enzymes (matrix metalloproteinases), which contributes to its effective biodegradation. To carry out photoinduced crosslinking by the mechanism of radical chain polymerization, methacryloyl groups are introduced into gelatin (by esterification with methacrylic anhydride). Gelatin can also be

modified with reactive groups that enter into radical thiol-ene reactions. For example, Bertlein *et al*.[50] introduced allyl groups using the reaction of glycidyl ether with gelatin at 65 °C in an alkaline medium. Van Hoorick *et al*.[51] synthesized gelatin derivatives with norbornene by reacting the primary amino groups of protein with 5-norbornene-2-carboxylic acid upon activation with carbodiimide. Both modifications provide polymer capable of reacting with multifunctional thiol crosslinkers to form a hydrogel. To incorporate desired biomolecules into the gel or to perform chemical crosslinking, gelatin can be functionalized with thiol groups.[52]

Hyaluronic acid (HA), which is an endogenous polysaccharide consisting of repeating unbranched units of glucuronic acid and *N*-acetylglucosamine, causes significant interest. Hyaluronic acid is found in many connective tissues and is involved in a number of biological processes, such as wound healing, maintaining tissue homeostasis, *etc*.[53] The prospects for using HA to create scaffolds in 3D photopolymerization are associated with the possibility of its degradation in the body under the action of hyaluronidase and oxidizing agents, as well as with its easy modification due to the presence of carboxyl and hydroxyl groups in the structure. For instance, methacrylate units were introduced into HA by a polymer-analogous reaction with methacrylic anhydride[54] or glycidyl methacrylate in the presence of triethylamine.[55] Hyaluronic acid, like gelatin, can be modified with norbornene by the reaction of 5-norbornene-2-carboxylic acid with hydroxyl groups[56] or by the reaction of 2-methylamino-5-norbornene with carboxyl groups.[57] However, the modification of the carboxyl group in HA was shown[58] to decrease the acid ability to interact with cellular binding sites, such as CD44. For this reason, the methods have been developed to maintain the concentration of carboxyl groups, for example, by interacting the HA hydroxyl groups with cysteines.[59] Such HA derivatives afford the preparation of hydrogels with a wide range of degradation times and with the most diverse architecture, which significantly expands the range of TECs created.

Chondroitin sulfate is proteoglycan found in connective tissue such as cartilage and synovial fluid. This biomolecule can be degraded by the action of enzymes. An important property of chondroitin sulfate is the possibility of its modification by introducing vinyl groups, for example, by reaction with glycidyl methacrylate in the presence of dimethylaminopyridine, proceeding through the formation of a salt with tetrabutylammonium.[60]

Other materials of natural origin can also participate in 3D photopolymerization: dextran, silk fibroin, collagen, decellularized extracellular matrix, alginate, κ-carrageenan, and chitosan. Such biopolymers can be modified by polymer-analogous reactions or by interaction with functional compounds capable of participating in the photoinduced crosslinking. For example, to introduce vinyl groups into dextran, it is reacted with methacrylic anhydride,[61] while for the modification of silk fibroin, it is reacted with glycidyl methacrylate in the presence of lithium bromide at 60 °C.[62] Methacrylate units are introduced into chitosan through interaction of hydroxyl groups with activated carbonyldiimidazole.[63]

The advantage of natural materials in 3D photopolymerization concerns the formation of hydrogels, characterized by high efficiency in cell encapsulation, biological activity, ability to degrade. They possess minimal immunogenicity, and contain functional groups responsible for the introduc-

8 of 26

A.N.Generalova, P.A.Demina, R.A.Akasov, E.V.Khaydukov
Russ. Chem. Rev., 2023, **92** (2) RCR5068

tion of photopolymerizable units. The wide use of natural polymers is limited by unpredictable molecular mass distribution and variation of properties for each batch, which impedes the control of mechanical parameters and the rate of biodegradation of the formed scaffolds.

3.1.2. Synthetic precursors of tissue engineering constructs

Synthetic materials, in contrast to natural compounds, allow the formation of hydrogels with well-reproducible properties and ability to control network formation, gelation kinetics, degradation rate, and mechanical properties. Hydrogels based on synthetic materials can be obtained by 3D photopolymerization from acrylate- and methacrylate-based monomers and oligomers by the mechanism of radical chain polymerization and redox polymerization (see Sections 2.1, 2.3), as well as from thiol-containing monomers and norbornene, *N*-vinylamides, vinyl and propyl esters of organic acids, maleimide, *etc.* by the mechanism of radical thiol-ene reactions (see Section 2.2).

Among synthetic polymers employed for hydrogel formation, polyethylene glycol (PEG) is the most widely used. This polymer is characterized by high hydrophilicity and low protein adsorption, which determines the long circulation time of structures based on this polymer in the circulatory system *in vivo*.[64] An important property of PEG is the possibility to incorporate vinyl moieties by utilizating simple methods. For example, the reaction of PEG with acrylic or methacrylic acid chlorides in the presence of triethylamine allows introduction of end acrylate or methacrylate units, which can enter into 3D photoinduced crosslinking by the mechanism of radical chain polymerization.[65] The hydrolytic degradation of PEG-based hydrogels is ensured by the introduction of α-hydroxy acids between the vinyl groups and the main PEG chain.[66] Polyethylene glycol can also be modified by end thiol groups or norbornene fragments to carry out thiol-ene crosslinking.[27]

Polyvinyl alcohol (PVA) is actively used for hydrogel preparation due to PVA hydrophilicity and the presence of hydroxyl groups, which can be easily modified. Fragments with vinyl groups are introduced in PVA, similar to natural polymers, via the esterification with methacrylic anhydride.[67] Modification of PVA with tyramine units, which is carried out by interaction of carboxylated PVA derivatives with tyramine under carbodiimide activation promotes the formation of hydrogels in the redox radical 3D-photopolymerization.[68]

Polylactide (PLA), as well as copolymers of lactide with glycolide (PLGA) and polycaprolactone (PCL) are examples of polymers that provide mechanically strong, biocompatible and biodegradable scaffolds. Different ratios of PLA and PLGA determine the hydrophilicity and regulate the rate of hydrolytic degradation, since PLA containing a methyl group decomposes slower than PLGA.[69] To increase the hydrophilicity and to control the mechanical properties of the material, it is copolymerized with PEG[70] or polyethylene glycol dimethacrylate.[71] Introduction of units with double bonds into such polymers, for example, by interaction with methacrylic anhydride, results in the formation of porous materials of a gyroid structure, which can function as soft tissue scaffolds.[72]

Synthetic polymers are also used to increase the strength of photocurable materials by improving homogeneity and controlling the crosslinking degree.[73] For example, flexible-chain polymers — polysiloxanes — have shown great

potential for achieving this goal. The addition of polysiloxanes, which, along with chain flexibility, have the ability to reduce surface tension, leads to a change in adhesion, morphology, surface energy, thermal stability, mechanical properties, and hydrophilicity of scaffolds. Advincula and co-workers[74] proposed a method for performing 3D photocopolymerization of oligomers of methacryloxypropylmethylsiloxane and methacrylate. The scaffold consisting of this composition was characterized by high tensile strength, good elasticity, and high compressive strength.

Despite a number of advantages of synthetic material, a significant disadvantage of such scaffolds obtained from them is low adhesion and weak cell proliferation on the surface and in the bulk. For this reason, the modification of the polymer surface is developed to improve its adhesive properties by incorporating adhesive proteins or peptides (*e.g.*, RGD peptide)[75] or molecules with heparin-binding sites.[49]

In general, synthetic polymers do not have the biological activity of natural materials; therefore, hybrid ink, which includes both natural and synthetic polymers,[67] is often used (see Section 5.2).

3.2. Initiators and radiation sources

Initiating systems based on one-, two-, or multicomponent photoinitiators play a key role in photopolymerization, which can proceed both via the radical and cationic mechanisms (the latter is not considered in this review).

Photoinitiating systems not only determine the reaction mechanism, but also affect its patterns, the rate, and the final properties of the polymer, such as hardness and viscosity. The main parameters of photoinitiator selection are the maximum absorption wavelength and the molar extinction coefficient. The efficiency of a photoinitiator relates directly to its structure, which determines the absorption range and quantum efficiency of photochemical and photophysical processes involving reactants in excited states.[76] Regardless of the type and mechanism of initiation, a photoinitiator should have the following properties:

— absorption wavelength falls within the emission band of the source;

— high quantum efficiency;

— good solubility in photocomposition;

— lack of cytotoxicity;

— high thermal stability;

— storage stability.

In addition, the course of photopolymerization is affected by the structure and physicochemical properties of the initial monomers (oligomers, macromonomers), the presence of oxygen, stabilizers or other additives in the photocomposition; thickness of the irradiated layer, type and intensity of the radiation source. In the case of *in vivo* photopolymerization, it is important to use low toxicity initiators, especially when exposed to light. Free radicals formed during initiation can react with the main components of living cells — cell membranes, proteins, and nucleic acids — and cause damage.[77] Applying photopolymerization to the creation of three-dimensional TECs requires understanding of the initiation reaction mechanisms, which can maintain cell viability without loss of the method resolution.

Photopolymerization is initiated by light irradiation of a photoinitiator or photoinitiating system that converts photon energy into generation of reactive radicals.[78] The light source can be xenon lamps, mercury lamps, LEDs, or lasers.

A.N.Generalova, P.A.Demina, R.A.Akasov, E.V.Khaydukov
Russ. Chem. Rev., 2023, **92** (2) RCR5068

9 of 26

The source photon wavelength can be in the UV (190 – 400 nm), visible (400 – 700 nm) or even in the near-IR (700 – 1000 nm) range of the spectrum. This Section presents the main types of photoinitiating systems that are used in 3D photopolymerization; specific examples of radiation sources that can activate these systems are given in Section 5.

Photoinitiators activated by UV and visible light can be of two types. In the case of type I initiators, free radicals are formed during homolytic photodissociation of the initial molecule. Type II initiators include mainly the systems consisting of a photoinitiator- co-initiator pair. In such systems, the process of electron transfer or hydrogen atom abstraction, leading to generation of corresponding radicals or radical- ions, occurs under the action of light. Photo-polymerization can also proceed under NIR light, but in this case, the two-photon initiating systems or systems based on upconversion nanoparticles, in which resonant energy transfer occurs, are applied.

3.2.1. Type I photoinitiators

When absorbing light, photoinitiator molecules of type I transfer into an excited singlet or triplet state, which is accompanied by the homolytic bond cleavage. This photo-chemical decomposition generates free radicals, mainly by the Norrish type 1 reaction, which can initiate radical polymerization or crosslinking.[79] Any weak bond can be cleaved, but initiators that break up at the $C-C$ bond adjacent to the carbonyl group are most commonly used (α-splitting) (Fig. 5). To activate such a decay, UV radiation is required (Table 1). The first photocurable materials were obtained using benzophenone as an initiator excited with UV-vis light (253 nm).[80] The main limitations of the first photoinitiators were associated with their hydropho-bicity and, accordingly, poor solubility in an aqueous medium, as well as the necessity to use high-energy UV radiation, which can damage cells. The development of methods for the synthesis of water-soluble photoinitiators guided the growing interest in biomedical applications of photopolymerization, which is reflected in the increase in the number of scientific publications in this field.[7]
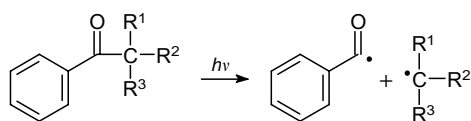

Figure 5. Type I initiator disintegration.

One of the main ways to increase the solubility of traditional radical photoinitiators is their chemical modifi-cation by introducing appropriate groups. They include nonionic groups of ethers, polyesters, hydroxyethers;[91] ionic groups of quaternary ammonium salts, sulfonates, carboxylic acids, and thiosulfates.[92] For example, the hydroxyethoxy group imparts hydrophilic properties to the initiator Irgacure 2959, which has been widely used in the last two decades for producing hydrogel TECs, and con-tributes to an increase in solubility in water [0.7 wt. (vol.)%]. Another advantage of using this compound is the absence of a cytotoxic photoreaction byproduct such as benzaldehyde.[81, 93]

Photoinitiator Irgacure 2959 absorbs in the UV spec-trum (200 – 370 nm) and dissociates with the formation of benzoyl and ketyl radicals. Unsaturated double bonds of monomers (oligomers, macromonomers) predominantly react with benzoyl radicals, which initiate radical chain polymerization or thiol-ene polycondensation.[94] However, light in the short-wavelength UV spectrum (< 300 nm) is phototoxic and mutagenic, which is unacceptable for experiments with cells. Therefore, to excite Irgacure 2959, a source with a wavelength of 365 nm, close to the visible light spectrum, is usually used, which reduces the efficiency of the reaction, since the molar extinction coefficient of Irgacure 2959 at this wavelength is rather low (only 4 mol L^{-1} cm^{-1}).[95] This makes it necessary to increase the irradiation intensity, exposure time and photoinitiator concentration during photoreaction.

At present, along with the modification of known initiators aimed at an increase in their solubility in water, the task is to expand the absorption range to create more efficient initiating systems.[96] Photoinitiators have been obtained, which include monoacylphosphine oxides and bis(acyl)phosphine oxides, absorbing in the wavelength range of 380 – 450 nm, and almost insoluble in water. One of the common photoinitiators of this series — diphenyl(2,4,6-trimethylbenzoyl)phosphine oxide (Daro-cure TPO) — has an absorption band in the range of 350 – 380 nm. However, even the energy of visible light (wavelength of up to 420 nm) is sufficient for the formation of radicals from such an initiator capable of inducing radical polymerization (see Table 1). In addition, Darocure TPO is uncolored and can be used to produce optically transparent 3D objects with high mechanical strength, which compares favorably with Irgacure 2959 mentioned above.[84]
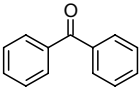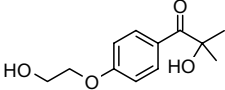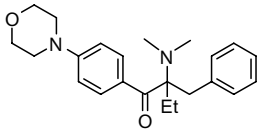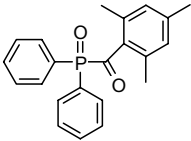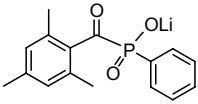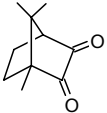
To obtain water-soluble initiators, TPO derivatives were synthesized, among which lithium phenyl(2,4,6-trime-thylbenzoyl)phosphinate (LAP) was widespread. This ini-tiator is highly soluble in water (8.5 wt.%) and has a high molar extinction coefficient (ε = 218 L mole^{-1} cm^{-1}) at a wavelength of 365 nm. The high efficiency of photoinitia-tion contributes to rapid formation of scaffolds on its basis.[97] This compound also weakly absorbs in the blue spectrum (λ = 405 nm, ε = 25 L mole^{-1} cm^{-1}). Thus, LAP is used to obtain 3D objects upon excitation with both UV and visible light in the process of radical chain polymer-ization and polycondensation.[11]

3.2.2. Type II photoinitiators

In the case of type II photoinitiators, as a rule, a more complex mechanism of initiation is implemented. The energy of photons in the visible spectrum, which is often used to activate such photoinitiators, is usually less than the dissociation energy of individual bonds in organic com-pounds. This significantly limits the choice of highly effec-tive initiators oper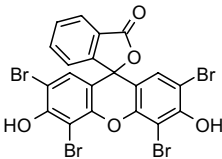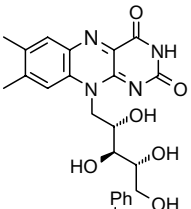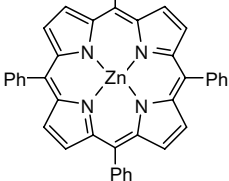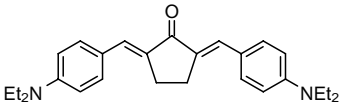ating in the visible range, and it is necessary to create two- or multi-component initiating systems containing an initiator and co-initiator. The activa-tion of type II initiators proceeds slower and less efficiently in comparison with initiators of type I, which is associated with the presence of competitive reactions involving the monomer, co-initiator, and atmospheric oxygen.

To date, multicomponent photoinitiation systems based on electron transfer and hydrogen atom abstraction, as well as systems that include both processes, have been developed to obtain the corresponding radicals or radical ions that initiate photopolymerization.[17] Electron transfer occurs upon interaction of an excited electron donor or

10 of 26

A.N.Generalova, P.A.Demina, R.A.Akasov, E.V.Khaydukov
Russ. Chem. Rev., 2023, **92** (2) RCR5068

Table 1. Examples of photoinitiators for 3D photopolymerization.

Title	Structural formula	Wavelength,[a] nm	Photopolymerization mechanisms	Ref.
		Type I initiators		
Benzophenone		253	Radical chain, thiol-ene reactions	17, 80
2-Hydroxy-1-[4-(2-hydr-oxyethoxy)phenyl]-2-methylpropan-1-one (Irgacure 2959)		274 (365)	Radical chain, thiole-ene reactions	81
2-Benzyl -2-(dimethylamino)-1-(4-morpholinophenyl)-butan-1-one (Irgacure 369)		365 (420) 800	Radical chain, thiol-ene reactions Two-photon polymerization	82 83
(Diphenylphosphoryl)-(mesityl)methanone (Darocure TPO)		350 (420)	Radical chain	84
Lithium phenyl (2,4,6-tri-methylbenzoyl)phosphinate (LAP)		375	Radical chain, thiol-ene reactions	11
		Type II initiators		
Camphorquinone		475	Radical chain, thiol-ene reactions	85
Eosin Y		525	Radical chain, thiol-ene reactions Two-photon polymerization	86 15
Riboflavin		450, 475	Radical chain	82, 87, 88
Zinc *meso*-tetraphenyl porphyrin (ZnTPP)		420	Controlled radical polymerization	89
		Two-photon initiators		
2,5-Bis[4-(diethylamino)-benzylidene]cyclopentan-1-one (BDEA)		750 – 800	Two-photon polymerization	90

[a] The absorption maximum is indicated; the working wavelength, which is used to activate photoinitiators, is given in parentheses.

acceptor (in the triplet state) with the second component (electron acceptor or donor, respectively) in the ground state (Fig. 6). In some cases, it is possible to quench the triplet state of the photoinitiator by the monomer, but the main way of radical formation proceeds through interaction with co-initiators.

Most often, amines are used as co-initiators due to their reducing properties. It is believed that the mecha-nism of such a reaction is based on interaction of amines with the photoinitiator in the excited state due to electron transfer with the formation of an intermediate ion pair (or exciplex) in the form of the photoinitiator radical anion
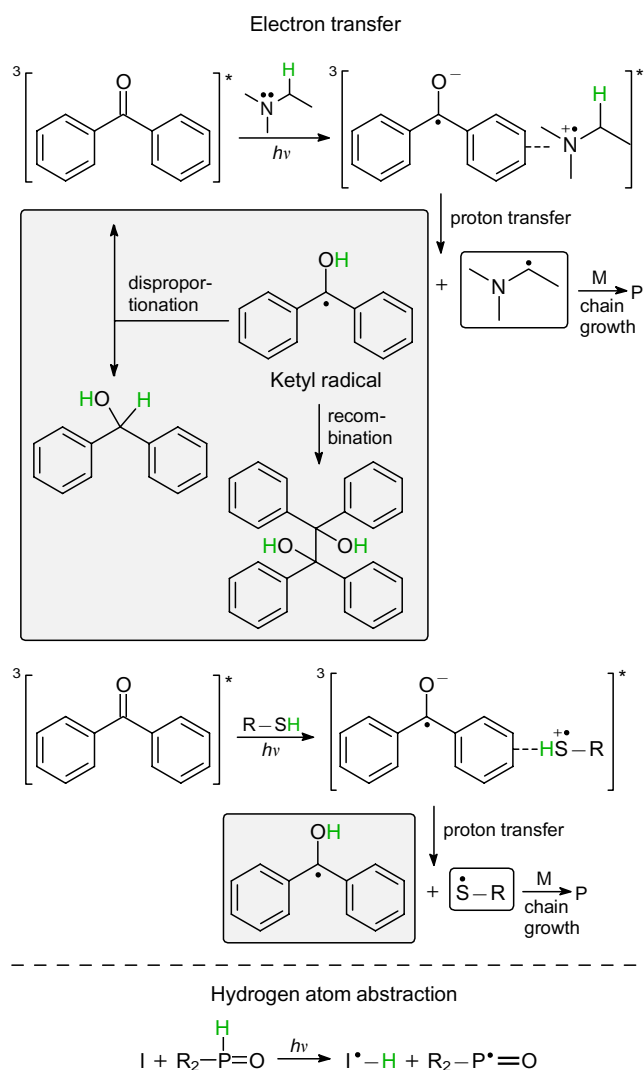
A.N.Generalova, P.A.Demina, R.A.Akasov, E.V.Khaydukov
Russ. Chem. Rev., 2023, **92** (2) RCR5068

11 of 26

Figure 6. Schemes of initiation with type II photoinitiator (benzophenone) *via* electron transfer (with amine and thiol as co-initiator) or hydrogen atom abstraction.

and the amine radical cation.[98] Then, proton transfer occurs with the formation of an active radical from an amine-based co-initiator and a photoinitiator ketyl radical, as it is shown in the example in Fig. 6. The ketyl radical is inactive with respect to the double bond and is deactivated by recombination with another radical or by a disproportionation reaction. As a result, the process of radical chain polymerization is initiated by co-initiator (amine) radicals.

Other types of co-initiators are also described in the literature. For example, thiols, which are involved in photo-induced electron transfer followed by proton transfer and the formation of free S-centered radicals capable of attaching to double bonds and initiating radical polymerization (see Fig. 6), have found wide application (see Fig. 6).[99] S-radicals are very active, insensitive to the inhibitory action of oxygen, and can attach to both vinyl and allyl groups. An important role of thiols is associated with their participation in photoinduced radical thiol-ene polycondensation reactions used to form hydrogels.

Phosphorus-containing compounds can also act as co-initiators in photopolymerization, acting as an electron or hydrogen atom donor. In particular, Lalevée *et al*.[100] showed that an excited photoinitiator can cause the abstraction of a hydrogen atom from a phosphorus-containing compound with a labile hydrogen−phosphorus bond (see Fig. 6). Such a path of the reaction without an electron transfer stage was proved via the spectral method by the absence of an intermediate ion pair.

One of the most widely used type II photoinitiators is bornane-2,3-dione, called camphorquinone (see Table 1). This compound is usually part of an initiating system with tertiary amine such as ethyl 4-(dimethylamino)benzoate when excited with visible light. Camphorquinone has been successfully used to prepare hydrogels with encapsulated viable cells,[85] but its low solubility and reactivity in water, as well as the yellow color of polymerization products, limit its application in most 3D printing technologies.

Dyes are of great interest as photoinitiators for visible light-driven polymerization. Such compounds are usually highly soluble in water and can participate in electron transfer reactions from an excited state molecule to a suitable co-initiator capable of triggering the photopolymerization process as a result of activation (see monograph,[101] p. 48). Dyes in the excited state act either as reducing or oxidizing agents, and their reaction with co-initiators proceeds through redox stages due to electron transfer. Most often, eosin Y, methylene blue, rose bengal, erythrosin are used in photopolymerization.[15] For instance, eosin Y, which was first used to initiate photopolymerization, has $\varepsilon = 60\,803$ L mole^{-1} cm^{-1} at the wavelength of 539 nm and it rapidly transforms into the triplet state when irradiated. When interacting with an amine-based co-initiator, for example, with triethanolamine (TEA), a hydrogen atom is abstracted and the deprotonated TEA radical initiates the chain and thiol-ene radical reactions. However, these processes are rather slow and require additional accelerators such as *N*-vinylpyrrolidone or *N*-vinylcaprolactam. The main disadvantage of eosin Y is the need to use a large number of components in the initiating system, which hampers optimization of the process.[86] The possibility of using eosin Y without participation of a co-initiator was demonstrated [102] using a successful example of a photo-induced crosslinking reaction of hyaluronic acid containing tyramine units by the redox mechanism with formation of dityramine bridges (see Section 2.3).

Some works have demonstrated the great potential of riboflavin (vitamin B2) as a type II initiator. This water-soluble biocompatible compound does not exhibit a cytotoxic effect and has a broad absorption spectrum with four maxima at 223, 267, 373, and 444 nm, which makes it particularly attractive as an alternative to synthetic initiators.[82, 87] To initiate radical polymerization by the redox mechanism, riboflavin requires the presence of a co-initiator as an electron donor. Various riboflavin-based initiating systems have been developed to prepare methacrylate hydrogels involving triethanolamine [87, 103] and L-arginine.[88] The degree of formation of riboflavin radicals and, consequently, the reaction rate depend strongly on pH of a photocomposition. In addition, it has been proven that after irradiation with UV or visible light in the presence of oxygen, riboflavin produces such reactive oxygen species as hydroxyl radical, peroxide radical anion, singlet oxygen, *etc.* This effect can significantly accelerate initiation of photopolymerization (see Section 2.3).[35]

The photochemical properties of metal complexes, in particular, strong absorption in the visible range, relatively

long-living excited states, and suitable redox potentials determine the possibility of participating these compounds in redox processes (see Table 1). First of all, they can be used in controlled radical chain transfer polymerization by the addition-fragmentation mechanism (AFTP, RAFT) (see Section 2.4). For example, such processes actively employ an initiating system based on complexes of tris(2,2′-bipyridine) dichlororuthenium(II) (Ru) hexa-hydrate ($\varepsilon = 14\,600$ L mole^{-1} cm^{-1} at 450 nm). Irradiation with visible light excites the ground state of Ru^{2+} ion, which is oxidized to Ru^{3+} by transferring electrons to a co-initiator such as sodium persulfate. After accepting electrons, persulfate dissociates into sulfate anions and sulfate radicals capable of triggering radical chain polymerization or thiol-ene polycondensation.[104] The zinc *meso*-tetraphe-nylporphyrin (ZnTPP) photosensitizer, used in photody-namic therapy of cancerous tumors, also seems interesting (see Table 1).[89] An effective system for initiating radical chain polymerization of hydroxyethyl methacrylate upon irradiation with light at a wavelength of 420 nm was obtained through combination with diphenyliodonium complexes.[105] Despite the great potential, the use of these systems is limited due to the presence of a metal in their composition, which may have a toxic effect, and low storage stability.

3.2.3. Initiating systems activated by near-IR light

In comparison with UV and visible light, NIR radiation does not lead to strong photodamage of the material, has low scattering in tissues and a large penetration depth. One of the possible ways of 3D photopolymerization under the NIR light action is based on the use of two-photon polymerization (2PP). This process is similar to traditional single photon polymerization based on absorption of a single photon. However, in the case of 2PP, high-intensity laser radiation is used to trigger nonlinear absorption of two photons from the NIR spectrum (~ 800 nm) which leads to the molecule transition through a virtual energy level into an excited state.[106] The energy difference between the ground and excited states is equal to the sum of energies of two photons (Fig. 7 a,b). Since in this case the energy of molecule transition to an excited state is in a quadratic dependence on the incident light intensity, 2PP allows creation of finely tuned objects at the micro- and nanolevels with a resolution of < 100 nm in the depth of photo-composition at a relatively high printing speed.[108] As a rule, femtosecond laser radiation is used to implement the 2PP process. It should be noted that the main technological development for biomedical applications of the 2PP method was owing to the efforts of a scientific team led by Prof. B.N.Chichkov, first at the Laser Center Hannover (Germany), and then at Leibniz University Hannover (Germany).

The use of low-energy photons, which are safe for cells, determines the possibility of 3D structure formation in the presence of living cells as well.[109] Initiators of two-photon polymerization should have low absorption at the working wavelength and also contain conjugated systems of π-electrons and groups with strong donor-acceptor properties in the structure (see Fig. 7 c). After photon absorption, an electron in the initiator is probably transferred from the donor-acceptor group to the π-system. The transfer of an electron from the initiator to the monomer generates exciplex (excited state) and leads to the formation of radicals that initiate polymerization.[110]
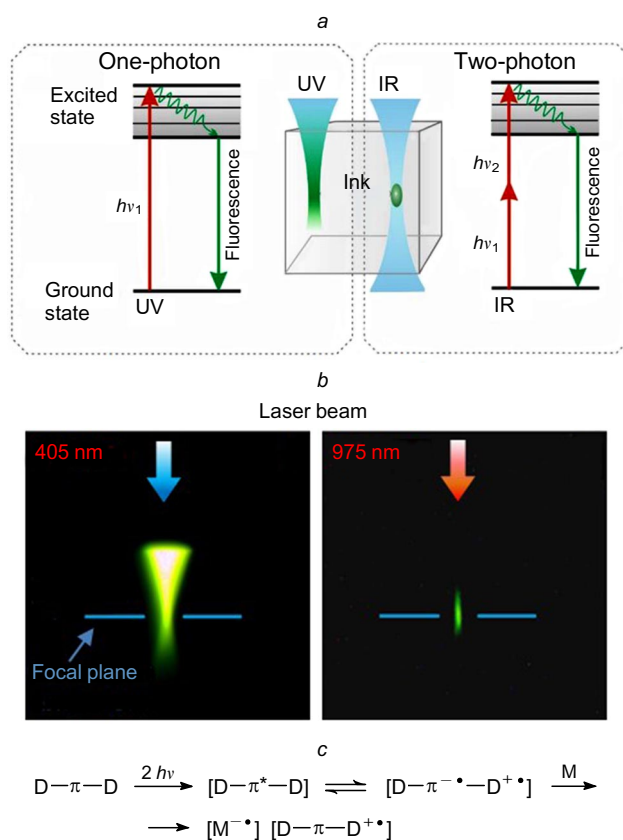

Figure 7. Energy diagrams of initiator excitation: schematic (*a*) and fluorescence (*b*) images of beam focusing in ink for one-photon (left) and two-photon polymerizations (right),[107] as well as the mechanism of two-photon polymerization initiation (*c*).

Two-photon polymerization uses type I initiators capable of homolytic decomposition upon irradiation, such as LAP. However, such compounds are characterized by relatively low π-conjugation and weak two-photon absorption that determines insufficient efficacy in the processes with excitation by IR-radiation.[111] Chichkov *et al.*[83] reported the use of Irgacure 369 as an initiator for two-photon polymerization. However, the small absorption cross-section in the IR spectrum and the absorption max-imum at a wavelength of 369 nm were the reason for insufficient efficiency of this photoinitiator irradiated by a laser source with wavelengths of $750-800$ nm.[112]

Some well-known type II initiators, such as eosin Y, erythrosin, and rose bengal, in combination with amines, have been successfully used as two-photon polymerization initiators.[15] However, these systems have the long process time and the high dose of irradiation, therefore, the task was to create initiators that ensure fast photopolymeriza-tion at low intensity of laser radiation. Specially synthesized water-soluble derivatives of chromophores, for example, 1,4-bis(4-{*N*,*N*-bis[6-(trimethylammonio)hexyl]amino}styryl)-2,5-dimethoxybenzene (WSPI) tetraiodide[113] and (2,5-bis[4-(diethylamino)benzylidene]cyclopentan-1-on (BDEA) showed high efficiency in two-photon polymerization (see Table 1).[90] Chesnokov and co-workers[114] demonstrated a relatively high polymerization rate at low NIR excitation power for imidazole-containing compounds with phenan-throline and phenanthrene fragments, used directly as two-

A.N.Generalova, P.A.Demina, R.A.Akasov, E.V.Khaydukov
Russ. Chem. Rev., 2023, **92** (2) RCR5068

13 of 26

photon polymerization initiators and in combination with amines.

Along with the great advantages of NIR radiation and the fabrication of high-resolution products, one of the significant limitations of 2PP is expensive equipment, namely femtosecond laser systems, which somewhat hinders the development of this technology.

Hybrid organo-inorganic structures are considered to be promising initiating systems excited by IR radiation. The mechanism of such structure action is based on the resonant energy transfer between the components. Successful examples of using upconversion nanoparticles (UCNPs) as inorganic components are presented in the literature. In these nanoparticles, low-energy NIR radiation (975 nm) is converted into UV (360 nm), visible (450, 475 and 650 nm) and NIR (800 nm) light with higher energy through real energy states of trivalent ions of rare earth elements.[115] UCNPs can be excited by CW radiation from cheap semiconductor lasers with a relatively low intensity (several orders of magnitude lower than in the case of a two-photon process). Together with UCNPs, traditional photoinitiating systems can be exploited to create 3D structures. This process occurs only if the UCNP emission spectrum overlaps with the absorption spectrum of the photoinitiator.

For example, UCNPs doped with Tm^{3+} ions were used as a source of UV light when irradiated by a laser with a wavelength of 980 nm. Overlapping of the UCNP emission band (360 nm) with the absorption band of the photo-initiator Irgacure-819 was the main condition for the initiator activation and the generation of radicals during polymerization. This hybrid initiator system allowed formation of 3D structures from an optically transparent polyethylene glycol diacrylate oligomer.[116] In addition, the structures of UCNPs with the Irgacur 369 were employed for crosslinking reaction of methacrylated oligocarbonate, as well as the structures of UCNPs with the Darocure TPO photoinitiator were employed for photocuring of the commercially available E-shell 300 resin.[117]

4. 3D printing for tissue-engineered constructs

Additive technologies, known as 3D printing, have been used since the 1980s to produce specific complex objects without using mechanical processing or special molds.[118] The application field of such processes is constantly expanding, covering a variety of areas, including biology and medicine.[119] In particular, 3D printing technology, which includes both rational design and production of TECs, plays a leading role in tissue engineering.[120] A special position is occupied by 3D printing, based on the polymerization or light-driven ink crosslinking. During irradiation, curing occurs, which allows easy and quick separation of the object from the original liquid composition. In this review, when describing technologies, the term photocuring will be used, which implies the crosslinking or polymerization. Photoinduced processes are characterized by a high spatiotemporal resolution, they proceed with a minimum amount of byproducts, and allow creation of the required three-dimensional structures from monomers (oligomers, macromonomers), cells, and biologically active molecules. Great opportunities of 3D printing are associated with the formation of multifunctional 3D objects of various architectures with controlled chemical, optical, and mechanical properties.[12]

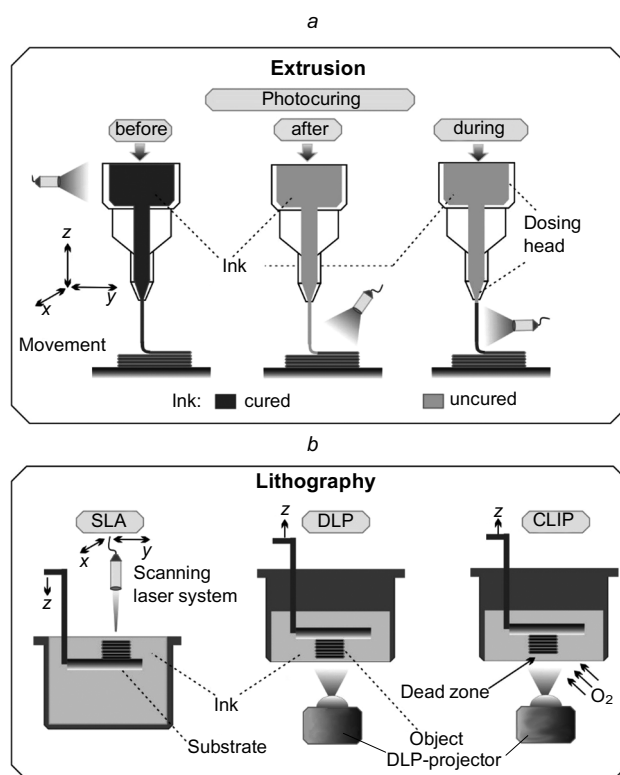Usually the process of 3D printing includes three stages:

Figure 8. Schematic representation of extrusion-based 3D printing technologies involving inkcuring before, after and during extrusion (*a*), and lithography (*b*). SLA is stereolithography, DLP is digital light projection, CLIP is continuous liquid interface production. The figure is created by the authors.

1) design of 3D-structures by means of computer simulation;

2) presentation of 3D-structures in the form of layers;

3) sequential printing of layers resulting in the 3D structure formation.

As it was noted above, two main approaches are used to obtain 3D TEC models (Fig. 8):

— printing by extrusion, based on a photoreaction activated by light before, after or immediately upon photo-composition exit from the extruder;

— printing based on lithography, when a photoreaction occurs in a layer of a photocomposition irradiated with light.

These methods provide structurally organized functional TECs for various biomedical purposes.[12]

4.1. Extrusiuon-based 3D printing

The principle of extrusion printing consists in pressing ink through the nozzle and forming the layers that make up the product on the platform using a computer created design. The deposition of each subsequent layer of ink occurs by moving either the extruder above the platform or the platform below the extruder. As a result, three-dimensional objects are created by continuous layer-by-layer application of material. In the case of 3D printing, ink after the extruder is irradiated with light to form hydrogels. The object can be illuminated in different positions between the nozzle and the platform, starting from the nozzle outlet and ending with irradiation directly on the platform (see Fig. 8 *a*). A typical extrusion 3D photoprinter consists of a dosing head, which can move along two axes and a platform where photocured

14 of 26

A.N.Generalova, P.A.Demina, R.A.Akasov, E.V.Khaydukov
Russ. Chem. Rev., 2023, **92** (2) RCR5068

ink is deposited.[121] The ink is supplied mechanically (by piston) or pneumatically (by air pressure) through the nozzle with small holes (dies) (see Fig. 8 *a*).[122]

Successful extrusion 3D printing is grounded on the ink requirements, specific for the technology, which determine the possibility of given composition extrusion and its high-precision deposition to reproduce the desired 3D structure. First of all, the rheological properties of ink should allow it to pass through the printhead, usually having a nozzle diameter of $100-800$ μm, which is optimal for dosing the material. Constriction of the nozzle and corresponding high shear stresses that occur in the nozzle are the reasons for the preferred use of ink with low viscosity for layer-by-layer deposition. However, finished scaffolds must maintain integrity, shape and structure under the action of external forces. Ink consiting of high-viscose materials or with high-polymer content can be used to produce structures with high resolution and precision, and the balance of these properties must be maintained in such a way that the viability and function of the cells included in the material are not reduced.[123] Various approaches to scaffold formation are developed that meet the structural requirements along with presevation of the biological activity of cells. In particular, these approaches include layer-by-layer deposition and total irradiations of the entire structure,[124] ink crosslinking prior to extrusion,[125] the use of additives that give the products the properties of a non-Newtonian liquid (with low viscosity in the dosing head and with high viscosity when leaving the nozzle),[126] ink deposition into supporting moulds,[127] *etc*.

One of the promising approaches to extrusion 3D printing is photocuring of the composition during extrusion (*in situ*) (see Fig. 8 *a*). In contrast to processes involving crosslinking reactions before or after extrusion, in the case of *in situ*, the formation of threads occurs after ink irradiation in a photopermeable capillary immediately after leaving the nozzle. This allows the use of a non-viscous ink without any additives or additional processing steps. Moreover, a homogeneous photocomposition is maintained, which determines the constant pressure in the dosing device and production of polymer structures of a given geometry at a high level of viability of encapsulated cells.[128, 129]

The technology of multi-jet 3D printing (MJP), which uses a printhead with an array of nozzles (from 96 to 448 pieces) is of great interest. This technology allows deposition of materials of various colors, hardness, strength, *etc.* on the substrate with a high resolution, providing a print layer thickness of 16 μm. However, MJP printers are expensive, as is the ink, which must have a low viscosity to be used in this technology.[130]

Based on extrusion, including multi-jet printing, the concept of 4D printing has been developed. This concept was first presented in 2013 using the example of creating products of complex configuration due to the shape memory effect.[131] The main feature of 4D printing is the ability to produce 3D objects that can change their shape, properties, or function over time in response to the action of such external stimuli such as temperature, light, water, *etc.*[132] In addition, this technology allows significant time and material saving when forming thin-walled or network structures,[133, 134] and also printing single- and multicomponent hydrogels.[135] A change in the shape of constructs is based either on the use of smart materials or on the creation of a localized self-deformation inside the printed object during or after printing.[136] 4D printing also provides maturation of

cell population in time when they are co-printed with hydrogels.[137] The main limitations of extrusion-based 4D printing are slow printing speed and relatively low resolution.

Currently, extrusion-based 3D printing is actively used to create TECs in a wide range of sizes: from small cellular hydrogel objects to complex anatomical structures, which cannot be achieved by other methods.[138] However, scaling affects the printing speed and leads to a relatively low resolution during production ($\sim 100-200$ μm).[139, 140] The last disadvantage can be eliminated by structural changes in the printer, for example, by reducing the nozzle diameter, although in some cases this may be accompanied by a lower rate of cell survival and clogging of hole in the nozzle.[141] Together with possibility of obtaining TECs of various sizes, the advantages of this method are the simplicity and availability of inexpensive commercial equipment, a wide range of suitable ink, including those with high viscosity, the possibility of incorporating cells at a significant concentration comparable to those for natural tissues, as well as minimal ink losses in the process of production.[12] To date, various types of tissues have been produced by extrusion 3D printing: bone,[142] cartilage,[143] cardiac,[144] and nervous tissues.[145]

4.2. Lithography-based 3D printing

Currently, there are a large number of 3D printing technologies that are based on the process of lithography: formation of two-dimensional objects on the ink surface. One of the first developed methods, actively and widely used both in biology and medicine, and in various industries, is stereolithography (SLA). This method was patented[146] in 1984 by Charles Hull, a co-founder of 3D Systems, a leader in 3D printing. In Russia, key competencies in the field of stereolithography were developed at the Institute of Problems of Laser and Information Technologies of the Russian Academy of Sciences under the guidance of Academician V.Ya.Panchenko.

The general principle of SLA is to scan the ink surface with a laser beam from a source (usually at a wavelength of 355 nm) located above (below) the tank. As a result of irradiation, the composition is photocured on the platform in the form of a layer, which is a cross-section of a 3D contruct. Then the platform is lowered (raised) by the thickness of the next layer and surface scanning with a laser beam is repeated (see Fig. 8 *b*). The process continues until a cured 3D construct corresponding to a computer model is obtained.[147] This technology allows resolution from 50 to 250 μm. The formation of each layer is controlled by the laser beam movement, which can occur over a large surface area and print constructs of a significant size (up to 50×50 cm) with little or no loss in performance precision.

Based on SLA, a masked stereolithography printing technology was developed; it consists in applying thin layers of ink according to a physical pattern or mask of the corresponding contour, followed by material irradiation with UV light. Irradiation causes material curing and removal of non-irradiated liquid composition from the work area. Recently, this method has been replaced by film transfer imaging (FTI) technology, which, thanks to introduction of digital projectors, has become almost analogous to digital image projection (DLP),[148] presented below. Stereolithography is devoid of some disadvantages of extrusion-based printing. For example, during the photo-

A.N.Generalova, P.A.Demina, R.A.Akasov, E.V.Khaydukov
Russ. Chem. Rev., 2023, 92 (2) RCR5068

15 of 26

curing process, no pressure is applied to the liquid composition leading to cell death. However, significant restrictions of this method are the insufficient choice of cell-laden ink,[149] and the fact that commercial SLA systems are mainly intended for the production of solid polymeric materials that do not meet the requirements of biomedicine.[150]

Among modern 3D printing technologies based on lithography, the DLP method and the liquid crystal display method (LCD) should be distinguished. The main difference between all lithographic technologies, including SLA, is the light source and visualization system with almost the same type of control system and layer-by-layer printing of 3D structures. In DLP technology, a layer of ink is cured with light from a DLP digital projector using a DLP matrix (usually from the tank base). This allows simultaneous irradiation of the entire polymer layer, creating objects according to the mask formed by the DLP matrix, in contrast to SLA technology, where point scanning occurs. This approach provides high resolution (10–50 m) at a higher printing speed compared to similar SLA parameters.[151] In addition, the DLP method uses visible light (405 nm) instead of UV radiation, incompatible with semiconductor materials of a DLP projector, which is especially important in the case of photocuring of compositions containing cells (see Fig. 8 b).[152] The use of a DLP matrix as a dynamic mask generator allowed the development of the projection micro-stereolithography method (PμSL), which was used to obtain complex 3D structures 0.6 μm in size under UV irradiation with a high resolution.[153]

However, simultaneous illumination of the entire layer is possible only for a limited area. At present, the size of the resulting layers varies from 100×60 to 190×120 mm. Therefore, DLP 3D printing is mainly used to print small objects with high precision.

The LCD printing technology is similar to DLP, but the mask is formed by the LCD matrix, which transmits the LED light only to the areas that need to be cured. The advantages of LCD printing are low cost and good resolution, but the light intensity is very low since only 10% of light can come from the LCD screen.[16]

Despite the great promise of the presented 3D lithography methods, there are problems that require the improvement of modern technologies. For example, the printing quality is reduced by the stair-stepping effect, since only flat layers with sharp edges can be produced.[154] A solution to this problem has been presented in the literature in the form of a technology called computed axial lithography (CAL). In this technology, radiation affects the entire volume of the printed product at once, in contrast to SLA technology, in which the effect occurs pointwise, or DLP and LCD methods, in which a two-dimensional layer is illuminated. Thanks to this feature, the CAL technology leads to a multiple acceleration of the printing process.[155]

Lithography-based 3D printing is also limited by the relatively low printing speed, caused by the low rate of photopolymerization and process discreteness (printing does not occur when the platform is moved). The new technology of continuous liquid interface production (CLIP) (see Fig. 8 b), based on continuous printing in a liquid medium, was developed in 2015 by Carbon 3D Corp.[156] This technology allows printing of more uniform structures 25–100 times faster than the conventional 3D

printing methods. The innovation of the method lies in the presence of a dead zone: a thin layer of uncured ink between the formed construct and the tank bottom. This zone is located above the base of the tank made of a specially designed membrane that transmits radiation from the source and oxygen, supplied from below. Projection irradiation by the DLP technology activates photocuring, and oxygen inhibits radical reactions, stably maintaining the presence of a liquid ink layer. This dead zone, whose size can be adjusted by the flow of oxygen, ensures the continuity of printing, i.e. at the moment the photocured layer is deposited on the 3D structure, the next layer of ink is irradiated.[150] Despite the advantages of this method, its efficiency can be fully achieved only for ink with low viscosity, which determines the rapid supply of material to the printing area, and when creating hollow structures that do not require a large amount of material.

Holographic 3D printing, or interference lithography, which uses two or more light sources to create an interference pattern is of great interest. By superimposing light waves, a pattern with a periodic structure is formed due to a local change in the light intensity.[157] This technology is well known in the field of creating nanostructured substrates, microframes, 3D photonic crystals, and microsieves.[158] Holographic 3D printing is a fast and accurate method for obtaining photocurable structures and, despite the limited number of templates, it is suitable for producing porous tissue contructs.[157]

One of the advanced technologies of stereolithography, distinguished by ultra-fast making of structures with sub-micron 3D resolution ($\sim$100 nm), is based on the 2PP process (see Section 3.2.3). In this technology, the initiating system responsible for polymerization is activated by a focused beam of a femtosecond NIR laser ($\sim$800 nm) due to nonlinear absorption.[159]

The main advantages of 2PP as compared to traditional single-photon polymerization include the possibility of producing three-dimensional images in the ink volume. This is due to the fact that IR light cannot initiate single-photon polymerization, while in the case of 2PP, initiation is possible, but only in the region of laser beam waist (voxel).[160] Thus, the laser beam can pass through the ink without polymerizing the material on its way and induce polymerization only in the focal volume. The strong nonlinear dependence of two-photon absorption on intensity allows localization of the region of photoreactions in ink near the voxel and unprecedented resolution of the method. The possibility of producing arbitrary three-dimensional structures is implemented by three-dimensional movement of the voxel over the photocomposition volume (see page 10 in Ref. 161).

The simplest 2PP-based setup consists of a laser source, focusing optics, a moving platform, and a 3D printing control system. Nanoscale resolution can be achieved by controlling the power density of the laser pulse and the printing speed. Traditional lithographic materials are usually used as photopolymerizable components in 2PP ink, but printing the products with nanoscale precision ($<$100 nm) is a relatively time-consuming process, which can hardly be implemented through other 3D printing technologies.[107]

Despite the numerous advantages of the 2PP-based technology, optical systems for such polymerization are currently still expensive. Products can be made only at high intensity of laser radiation (mainly on the order of

TW cm^{-2}) and from a single material, which excludes production of multifunctional structures.[120] In addition, the height of the printed construct is limited by micro-objective working distance used to focus the laser pulses in the ink.[162]

The development of lithography-based 3D printing is a particularly promising avenue in the creation of artificial bone grafts, since this technology has great prospects for making products with a complex structure and high resolution.[163] It should be noted that this technology provides the possibility to obtain not only porous structures, filled with cells or bioactive components, but also constructs simulating, for example, hollow vessels,[164] which are difficult to make using extrusion-based printing.

5. Biomedical applications

Successful application of photoinduced 3D printing technology in regenerative medicine for obtaining tissue-engineered constructs requires consideration of the requirements for cytotoxicity and immunogenicity of materials, as well as the correspondence of mechanical and chemical properties of the tissue in which scaffolds of this type are supposed to be used. Since the concept of photoinduced 3D printing implies the maximum convergence of photopolymerization process and cellular technologies, the most interesting are investigations with polymerization in the tissues of the body (*in situ* photopolymerization). In this case, the cells are introduced into the scaffold at the time of preparing photocomposition for a tissue bioequivalent and their subsequent autologous transplantation as part of such bioequivalents.

5.1. Cytotoxicity assessment

Cytotoxicity of materials and methods used is one of the most important factors that must be taken into account for the successful application of 3D printing technology. And if the scaffold material can be chosen in advance by selecting the most biocompatible materials for this purpose (see Section 3.1), then the toxic effect of the technology itself is much more difficult to assess (see p. 250 in monograph[165]). As it can be seen from the data given in Table 1, a number of photoinitiators are excited by UV light, which itself can induce photooxidative stress in the cell. The use of UV radiation is not a fundamental limitation for photopolymerization in living systems: for example, earlier LAP and Irgacure 2959 initiators were used to photopolymerize primary human chondrocytes in scaffolds based on methacrylated gelatin irradiated with 20-W LEDs ($\lambda = 405$ and 365 nm, respectively).[166] Cells retained their viability for 28 days, but the authors noted a decrease in cell viability by this time in all samples. An important problem in the use of initiators in any available spectrum range is the formation of radicals necessary to start photopolymerization processes. The generated radicals can seriously damage the structure of cellular biomacromolecules, and this principle underlies photodynamic therapy.[167] Sometimes, to protect cells, antioxidants, such as ascorbic acid[168] or hydrogen sulfide, are added to the photocomposition immediately before polymerization.[169] This approach allows an increase in the survival rate of encapsulated cells, but, in turn, it slows down the polymerization process.[168] In most cases, researchers make up with a certain number of cells that die during photopolymerization by choosing such cultures and photoinitiators to minimize this effect. In particular, chon-

drocytes,[170] fibroblasts,[171] mesenchymal stem cells,[172] and keratinocytes[173] (*i.e.* all the cell types most in demand in tissue engineering) tolerate photopolymerization well.

It should be noted that the inclusion of cells in the photocomposition can also affect the process of photo-crosslinking and lead to formation of inhomogeneities within the gel. It was shown that encapsulation of chondrocytes in a PEG-based composition followed by a crosslinking reaction during irradiation with a UV lamp [$\lambda = 352$ nm, excitation intensity (I_{ex}) = 5 mW cm^{-2}] caused a decrease in the bulk and local density of hydrogel, and thiol-mediated interactions between dithiol crosslinkers and free thiol groups on the cell surface played an important role.[174] This effect was more pronounced with increasing cell density during encapsulation. Encapsulation of chondrocytes in fluorescently labeled hydrogels resulted in formation of hydrogel with a density gradient around the cell, which was eliminated by treating the cells with estradiol antioxidant prior to encapsulation. During hydrolytic degradation of PEG hydrogel in the presence of cells, spatial density variations were also observed.[174]

The photopolymerization technology can also be used to encapsulate multipotent cells, which are extremely sensitive to environmental conditions. Thus, the composition on the basis of methacrylated glycol-chitosan and type I collagen had excellent biocompatibility at the example of reprogrammed multipotent cells. At that, the spread of cells and the formation of structures similar to muscle fibers occurred without undesirable osteogenic or chondrogenic differentiation, which was confirmed by gene expression analysis.[175]

Despite the fact that photoinitiators (Irgacure 2959, riboflavin) excited by UV- and blue-visible light were used in almost all the works mentioned above; cell survival was > 90%. The transition to photoinitiators activated by visible light in the green and red spectra allows both an increase in cell survival due to lower irradiation energy and light penetration to the depth of the photocomposition (biological tissue), which is beneficial for the photopolymerization process as a whole. Eosin Y, which has good solubility in water and low toxicity, often acts as such an initiator.[176] Structures obtained with its help under LED irradiation ($\lambda = 525$ nm, $I_{ex} = 5-100$ mW cm^{-2}) can support the functioning of mesenchymal stem cells while maintaining their ability to proliferate and differentiate.[177] However, it should be taken into account that an increase in the concentration of eosin Y in the photocomposition negatively affects cell viability and mechanical properties of hydrogel, its swelling coefficient, and porosity; *i.e.* cell adhesion. Thus, an increase in the concentration of eosin Y from 0.01 to 0.04 mole L^{-1} in a methacrylated gelatin-based photocomposition (GelMA) using the DLP technology (laser with $\lambda = 405$ nm and $I_{ex} = 48.6$ mW cm^{-2}) resulted in a decrease in the viability of mouse fibroblast cells NIH-3T3 from 91.5 to 75.6%, while the Young s modulus of compression increased from 4.40 to 14 kPa, and cell adhesion was maximum at eosin Y concentration in the composition equal to 0.04 mole L^{-1} (see Ref. 178).

A further development of this concept was the use of two-photon initiating systems (see Section 3.2.3), which, under the action of pulsed femtosecond radiation at a wavelength of 800 nm (80 fs at 75 MHz, power of 330 mW), allow printing of tissue bioequivalents with high cell viability.[179] However, in terms of abundance, two-photon systems are still inferior to photoinitiators in the UV and visible spectra. It should be noted that the require-

A.N.Generalova, P.A.Demina, R.A.Akasov, E.V.Khaydukov
Russ. Chem. Rev., 2023, **92** (2) RCR5068

17 of 26

ment for low phototoxicity of initiators becomes much more stringent when turning to *in situ* photopolymerization technology, *i.e.* directly in a living organism, as there is a risk of damage and mutation of cells of a person own tissues. Therefore, to implement this approach, the use of NIR radiation, deeply penetrating and neutral for cell, seems to be the most promising due to the technology of two-photon polymerization or participation of upconversion nanoparticles that transform the NIR radiation into visible and blue light.[180]

The search for new potential photoinitiators can proceed not only by applying irradiation from the transparency window of biological tissues, but also through the use of various nanocompositions that can perform several functions at once: photoinitiation and visualization or photoinitiation and drug delivery. For example, carbon nanotubes containing the anti-inflammatory drug formononetin, which is intended for the treatment of spinal cord injuries, have been proposed as such a nanocomplex. Nanocomposites were introduced into GelMA and irradiated with UV light ($\lambda = 365$ nm, $I_{ex} = 6.7$ mW cm^{-2}) to activate photopolymerization, while a short irradiation time (up to a minute) allowed the process to proceed without reducing cell viability (survival rate of $> 80\%$).[181]

It should be noted that cytotoxicity is the most important and easily detectable biocompatibility factor, but far from being the only one. Thus, adhesion of cells to a polymer is also important for the successful use of 3D printing technology, but the goals of increasing cell adhesion can be different. For example, in the case of a nanocomposite hydrogel containing GelMA, nanohydroxyapatite (nHAP), quaternized chitosan (QCS), and nanoparticles of functionalized polyhedral oligomeric

silsesquioxane (POSS), the goal was to improve cell adhesion to stimulate the regeneration of skull bones.[182] Irgacure 2959 and POSS nanoparticles irradiated by UV light ($\lambda = 365$ nm, $I_{ex} = 50$ mW cm^{-2}) served as a photoinitiating system and, together with hydroxyapatite and QCS, increased the mineralizing ability and cell adhesion. The prepared nanocomposite hydrogels had high mechanical properties and high cytocompatibility, including the ability to osteodifferentiate.

To achieve the opposite effect, Wang *et al.*[183] prepared ink based on PLA with monoethyl fumarate, *N*-vinylpyrrolidone, and Irgacure 2959 as a photoinitiator. UV irradiation at an Ultralum crosslinking cabinet ($\lambda = 365$ nm, $I_{ex} = 50$ mW cm^{-2}) led to formation of scaffolds with low cell adhesion, illustrated in mouse fibroblast culture L929. The resulting non-cytotoxic scaffolds can be used as antiadhesion barrier materials (for example, stents and any tubular structures).

5.2. Obtaining tissue-specific constructs

An important advantage of using photoinduced 3D polymerization technology in regenerative medicine is the possibility of obtaining complex structures with a given geometry and biomechanical properties. For example, a strategy for 3D bioprinting of a trachea using photocrosslinkable tissue-specific ink (Fig. 9) was recently proposed.[184] One of the main difficulties in creating a trachea bioequivalent is its heterogeneity: alternant cartilaginous rings and vascularized rings of fibrous tissue; it is also important to form the tracheal epithelium, which is necessary for implementation of the mechanical and physiological functions of the trachea. Since the trachea is a tubular organ, the requirements for the mechanical properties of
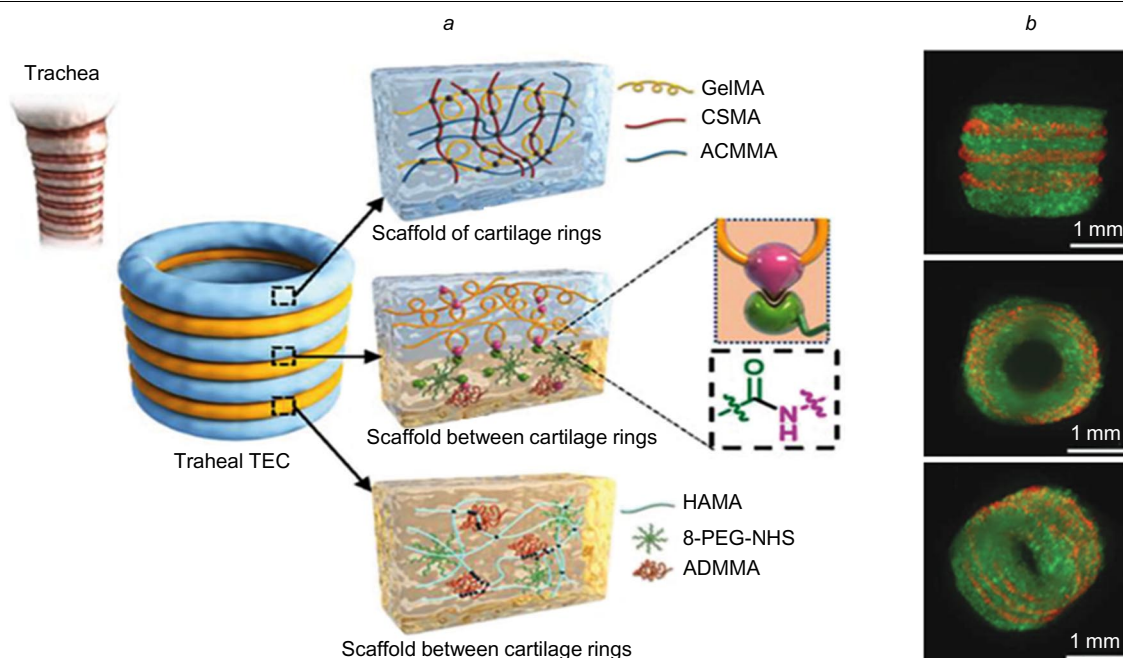

Figure 9. Schematic representation of tracheal TEC obtained by ink photopolymerization (to make scaffolds of cartilage rings and fibrous tissue) and amidation reaction (for interfacial binding) (*a*), and 3D images of cell distribution in tracheal TEC in three projections, made using fluorescence microscopy: chondrocytes labeled with green fluorescent protein (GFP) are stained green; fibroblasts labeled with red fluorescent protein (RFP) are stained red (*b*). GelMA is methacrylated gelatin, CSMA is methacrylated chondroitin sulfate, ACMMA is methacryloyl-modified cell-free cartilage matrix, HAMA is methacrylated hyaluronic acid, 8-PEG-NHS is polyethylene glycol succinic acid ester, ADMMA is methacryloyl-modified cell-free matrix of dermis. Adapted from paper.[184] The figure is published under the Creative Commons Attribution 4.0 International license (CC BY 4.0).

material are also high. The authors of the study[184] proposed alternant layer-by-layer printing with two types of ink: chondrocyte- and fibroblast-loaded ones. Photocrosslinkable ink of the first type consisted of methacryloyl-modified gelatin, chondroitin sulfate, and cartilage acellular matrix and was intended to create analogs of cartilage rings. The ink of the second type included methacrylate-modified hyaluronic acid, 8-arm-polyethylene glycol-succinic acid ester, and methacryloyl-modified derm acellular matrix, and it was suitable for reproducing a vascularized annulus fibrosus (see Fig. 9 a).[184] Polymerization under UV-LED irradiation ($\lambda = 365$ nm, $I_{ex} = 20$ mW cm^{-2}) occurring in both types of ink, and the amidation reaction for ring integration provided fast crosslinking with the formation of hydrogel networks, improved mechanical properties of material, high cell adhesion (see Fig. 9 b), as well as satisfactory specific tissue regeneration.

A similar task was associated with restoration of the intervertebral disc, a heterogeneous structure that consists of nucleus pulposus, annulus fibrosus, and two cartilage plates connecting adjacent vertebrae. To restore the intervertebral disc, hydrogel of methacrylated gelatin and hyaluronic acid, which allowed fixing the gelatin-like structure and triggering differentiation of mesenchymal stem cells characteristic of the nucleus pulposus, was obtained under the action of UV irradiation ($\lambda = 365$ nm, $I_{ex} = 7.0$ mW cm^{-2}).[185] It is important to note that photoinduced 3D polymerization for both cases presented above enabled flexible control of both the scaffold composition and structure and its mechanical properties, successfully combining the photopolymerization process with cellular technologies.

Currently, CLIP 3D printing technologies provide an opportunity to create structures with a complex architecture and required mechanical properties, including those infilled with cells and utilizing growth factors in photocompositions.[186] Imaging agents can be additionally introduced into the formed scaffolds for noninvasive monitoring of products after implantation. Ding et al.[187] made bioresorbable stents based on poly(1,12-dodeca-methylenecitrate) methacrylate containing a radiopaque compound, iodixanol, using a micro-CLIP printer ($\lambda = 365$ nm). The latter allowed stent detection in X-rays for at least 4 weeks after their formation and implantation. In addition, it has been found that the mechanical properties of stents can be controlled by changing the concentration of iodixanol.

Another difficulty is associated with the restoration of functional tissues, primarily the muscle ones.[188] It is shown that low-density GelMA hydrogels can be rapidly (< 1 min) formed under the action of visible light ($I_{ex} = 203$ mW cm^{-2}) and successfully used to encapsulate pluripotent human stem cells while maintaining their high viability. The initial stiffness of the resulting constructs is 220 Pa, even so they support cell growth and dynamic remodeling of the microenvironment, and also promote highly efficient ($> 70\%$) cell differentiation into cardiac tissue to obtain spontaneously contracting tissue-engineered constructs on the 8th day of differentiation.[189]

Deshmukh et al.[190] proposed another method for creating muscle structures based on a combination of acoustofluidics and photopolymerization. For example, muscle progenitor cells (myoblasts) were injected into gelMA-based hydrogels (5.0 wt.% GelMA and 0.1 wt.% LAP) and subjected to acoustic action to orient the cells into patterns corresponding to muscle fibers. Then, the cross-linking reaction was carried out under irradiation with a UV-LED ($\lambda = 405$ nm, $I_{ex} = 10$ mW cm^{-2}) focused with the help of a microscope objective. As a result, parallel strands, imitating the structure of skeletal muscles, were obtained and increased formation of myotubes and their spontaneous twitching were observed there. The authors believe that such an approach will allow the design of skeletal muscles, as well as tendons, ligaments, vascular networks, and their combinations thereof in the future.

An alternative option for creating patterns in hydrogels can be the introduction of scaffolds, for example, in the form of electrospun polycaprolactone fibers, into GelMA hydrogels.[191] To do this, polycaprolactone fibers and cells were added to the ink and polymerized. The mechanical properties of hydrogels containing such fibers were significantly higher than those of pure hydrogels. Encapsulated cells there grew faster as compared to conventional hydrogels. The authors attribute this effect to the texture of fibers, similar to the extracellular matrix, which can increase the biological activity of the material.

Photopolymerization also allows the creation of necessary patterns without introduction of additional components. A photopolymerizable biocompatible α-elastomer poly (glycerol sebacate) acrylate has been proposed for the development of an in vitro model of muscle regeneration and proliferation.[192] The mechanical properties of the construct were controlled by varying the light intensity during the DLP printing process ($\lambda = 385$ nm) to match the specific tension of the skeletal muscles. The formation of large-diameter channels and coating of extracellular matrix with proteins enhanced cell proliferation, and in vivo implantation of such a construct into a muscle tissue defect showed the promise of this technology. Li et al.[193] used the DLP technology ($\lambda = 405$ nm, $I_{ex} = 30$ mW cm^{-2}) to form the so-called multichannel nerve guidance conduits from GelMA with PC-12 cells, promoting the directed growth of axons to facilitate nerve regeneration, which is one of several clinical treatments for nerve conduction damage.

Printing of small tubular structures similar in size to blood vessels or glandular ducts is of great interest.[194] Recently, it was proposed to form such structures by extruding a hydrogel of methacrylate-modified hyaluronic acid, containing cells, directly into an aqueous solution of a photoinitiator (riboflavin + triethanolamine), which is excited by a semiconductor UV laser ($\lambda = 450$ nm, power of 900 mW) during scanning.[173] Diffusion of free radicals from the solution into the extruded structure initiated hydrogel crosslinking from the construct surface to the center. Thus, it was possible to form a crosslinked wall, whose thickness was determined by penetration of free radicals into the hydrogel volume.

Other approaches include utilization of dynamic DLP technology with an Omnicure S2000 UV curing system ($\lambda = 365$ nm), which allows production of three-dimensional branching vessel-like constructs with encapsulated cells, whose viability was maintained for at least 48 h after polymerization. However, this method requires significant engineering efforts and accurate calculation of the light dose at different depths of the hydrogel.[195]

Another example of an important and technically challenging biomedical application of 3D printing is retinal reconstruction. Recently, the two-photon photolithography of acrylated polycaprolactone loaded with retinal progenitor cells from induced human pluripotent cells has been proposed for this treatment.[196] Using the Nanoscribe Photonic

A.N.Generalova, P.A.Demina, R.A.Akasov, E.V.Khaydukov
Russ. Chem. Rev., 2023, **92** (2) RCR5068

19 of 26

Professional GT two-photon lithography system ($\lambda = 780$ nm) with direct 3D laser drawing allowed the obtaining of structures with a high resolution (up to 1 μm), which is very important in the case of retinal reconstruction. Such scaffolds supported the survival of retinal progenitor cells *in vitro*. Subretinal implantation of the resulting scaffolds in a porcine retinitis pigmentosa model did not cause inflammation, infection, and local or systemic scaffold toxicity after one month.[196]

In some cases, attention to photoinduced 3D polymerization is caused by the possibility of using tools designed to solve other problems in this field. So, polymerization lamps have proven themselves well in dentistry, for example, the VALO wireless dental lamp (Ultradent Products) with $\lambda = 395 - 480$ nm, which was proposed for regenerative dentistry using the GelMA composition with the LAP photoinitiator and encapsulated odontoblast-like cells OD21. During photopolymerization, $> 80\%$ of cells retained their viability, which, however, decreased with increasing light exposure time and increasing LAP concentration.[197]

5.3. 3D printing *in situ*

Bioprinting *in situ*, i.e. directly at the site of damaged tissue repair is a logical development of the technology of photoinduced 3D printing of tissue-engineered constructs, since it can provide minimal invasiveness and high accuracy of tissue reconstruction, including tissues with a complex structure. However, there are a number of difficulties, such as maintaining the ink composition under *in vivo* conditions, controlling the rheological and mechanical properties of the material, and time-limited printing. Some requirements for the resulting structures are internally contradictory: the synthesized constructs must, on the one hand, be strong enough to retain their shape for a long time, and on the other hand, they must be soft enough and capable of degradation so that the encapsulated cells can proliferate and perform therapeutic functions.[198]

Compositions based on PEG and Irgacure 2959 photoinitiator with introduced mesenchymal stem cells (MSCs) were injected into a cartilaginous defect of the rabbit knee joint under sterile conditions (3×2 mm in size) and photocured under UV light irradiation ($\lambda = 365$ nm, $I_{ex} = 5$ mW cm^{-2}).[199] In all cases, the hydrogel was easily formed in the defect without loosening or displacing from the chondral defect. During the experiments, chondrogenesis occurring in MSC cells and the ability of hydrogel to controlled uptake were confirmed, while the animals in the experimental group had the highest recovery rates.

One of the most significant restrictions in the transition to bioprinting directly in the body is the low light permeability of tissues, especially in the UV and blue spectra. The simplest solution to this problem is to use hydrogels to treat wounds and skin defects. Thus, a hydrogel based on hyaluronic acid with grafted groups of methacrylic anhydride and *N*-(2-aminoethyl)-4-[4-(hydroxy-methyl)-2-methoxy-5-nitrophenoxy]butanamide with introduced lyophilized amniotic medium was developed in 2022 to treat the diabetic wounds.[200] Irradiation with UV light using a LED ($\lambda = 365$ nm, $I_{ex} = 5$ mW cm^{-2}, LAP as a photoinitiator) resulted in hydrogel photocuring *in situ* within 3 s. At that, *o*-nitrosobenzaldehyde groups which can form a covalent bond with the amino groups of the tissue surface, were formed, and this ensured strong hydrogel adhesion to the tissue. It was shown that it significantly accelerated the healing of diabetic wounds by regulating macrophage polarization and promoting angiogenesis.

Irradiation through a fiber optic wire can be proposed as another approach to solving the problem of delivering light to the area of *in situ* photopolymerization. The success of this approach was demonstrated by injecting a photopolymerizable hydrogel containing mesenchymal stem cells into the nucleus pulposus of a rabbit intervertebral disc. The composition used included GelMA, LAP and MSC. After injecting this composition, a fiber optic wire was inserted into the disc space and irradiated with light at a wavelength of 405 nm at a power of 100 mW for 5 min. The results of magnetic resonance imaging (MRI) and histological analysis confirmed the success of this minimally invasive approach, although it was not possible to avoid the formation of osteophytes and defects. It is interesting that MSCs after irradiation showed increased anabolic activity, which may indicate a photobiological effect of light with $\lambda = 405$ nm.[201]

Utilizatiuon of IR and NIR light is optimal for biomedical applications, since it does not cause photodamage and, getting into the transparency window of biological tissue, it can deeper penetrate into it. This determines the intensive development of research related to the use of the IR spectrum for printing under *in situ* conditions. One of the first studies demonstrating the possibility of *in situ* photoinduced printing was the reconstruction of bone defects, in particular, the calvarium bones, using nanohydroxyapatite (n-HA) and a nanosecond pulsed laser emitting at a wavelength of 1064 nm.[202] It was shown that the ink material based on n-HA is biocompatible with osteoblast cells and does not cause inflammation *in vivo*, and the formed disks can start the restoration of a critical damage of the mouse calvaria bone (a hole of 4 mm in diameter) within a month. However, the insufficiently good mechanical properties of n-HA prevented healing in all cases, and later a more complex composition was proposed to solve this problem, including, in addition to n-HA, mesenchymal stromal cells and collagen.[203] Revascularization of the implanted area was implemented *via* laser printing with the help of the same laser. Obtaining the circulatory system of a given structure was achieved by applying red fluorescent protein(RFP)-labeled endothelial cells into a mouse calvaria bone defect, filled with collagen containing mesenchymal stem cells and vascular endothelial growth factor.[204]

A 3D printing technology using upconversion nanoparticles (UCNPs) in the presence of LAP was proposed in 2020.[180] In this case, UCNPs converted NIR laser radiation ($\lambda = 975$ nm) into light with a wavelength of 365 nm, which initiated polymerization in a DLP printer and formation of tissue-engineered constructs, including rather large ones, such as a human ear.

A similar approach was also proposed in work [205] for the restoration of soft tissues. The authors injected low-viscosity ink into the injury site through a thin needle, and polymerization was activated by UV-radiation of UCNPs, excited by NIR-light of a continuous-wave laser ($\lambda = 975$ nm, power of 9 W) using the DLP technology. Since the process was carried out using a focused beam, it was possible to carry out gradient photopolymerization, which allowed the control of both the mechanical and adhesive properties of the hydrogel by regulating the power of NIR irradiation and the concentration of UCNPs.

In the study,[206] three-dimensional photosensitive polymer hydrogels loaded with cells were printed using reactions of orthogonal two-photon cycloaddition and crosslinking of polymers under laser irradiation ($\lambda = 700 - 900$ nm, power of $0.7 - 2$ mW) with the help of a two-photon microscope (Scientifica 2-Photon microscope). This *in vivo* 3D printing of stem cells derived from donor muscles resulted in the *de novo* myofibril formation in mice. It is important that the *in situ* photoprinting technology allows formation of both microstructures (several tens of microns in size), for example, in the case of two-photon printing, and macrostructures. The latter are used, for example, to replace a full-layer cartilage defect in a model of a large animal (sheep) by printing discs with a diameter of 8 mm based on GelMA and a VA-086 photoinitiator, excited by an Omnicrue LX400 UV-LED ($\lambda = 365$ nm, $I_{ex} = 130$ mW cm^{-2}). This technique does not lead to postsurgical complications and ensures rapid cartilage regeneration.[207]

It should be noted that the technology of *in situ* photo-printing can be automated and robotized, which is important for further introduction of this method into clinical practice.[198] For example, a portable bioprinter that uses ink based on an aqueous two-phase emulsion containing GelMA and PEG was created.[208] The presence of two immiscible phases determined the possibility of pore formation, which promotes the transfer of liquid and oxygen, as well as cell proliferation. In addition, these TECs, while maintaining biocompatibility, were characterized by high elasticity and withstood multiple mechanical compressions. The 3D printing process was carried out in the presence of a LAP photoinitiator irradiated by five UV-LEDs ($\lambda = 365$ nm, $U = 4.2$ V, $I = 20$ mA). The presented bioprinter has been proposed to make wound dressings.

Another bioprinter was developed as a robot with six degrees of freedom and the ability of quick calibration to improve printing accuracy.[209] It allowed repairing an osteochondral defect (4×5 mm) in a rabbit joint within about 60 s with a printing error of < 30 m. The ink consisted of methacrylated α-hyaluronic acid and a crosslinking agent (branched PEG with terminal acrylate groups); a DLP printer with a UV laser from Prism (China) was used. It should be noted that for known bioprinters, despite the obvious problems with the depth of light penetration, it is typical to utilize UV initiators due to their availability and reliability.

It is important that the *in situ* printing technology allows creation of not only relatively inert biological structures (bones, cartilage, derm), but also muscles, for which functionality is important, in particular, the ability to contract. Thus, a handheld printer and ink that used a commercial Laponite® nanogel for controlled release of vascular endothelial growth factor (VEGF) and a GelMA-based hydrogel as a supporting scaffold were developed. As a result of curing under the action of a UV laser ($\lambda = 365$ nm), a scaffold with high cell adhesion was obtained (Fig. 10 *a,b*).[210]

It was shown that during direct UV-induced printing *in vivo* (see Fig. 10 *c*), the proposed composite was attached to skeletal muscles. At that, 7% GelMA in the composition provided a stiffness slightly lower than the stiffness of the rodent skeletal muscles, which allowed the scaffold to deform without destruction. In addition, this scaffold had a sustained release of VEGF, which promoted functional muscle recovery in a mouse model of quadriceps injury, reduced fibrosis, and improved anabolic response as com-

pared to untreated mice (see Fig. 10 *d*).[210] The GelMA-based composites demonstrated strong binding at the tissue − hydrogel interface due to hydrogen bonds and friction arising during photocrosslinking of composite materials, including heterogeneous ones (microgel + liquid precursor).[211]

As an interesting example of *in situ* photopolymerization, we can note an approach, when the required scaffold obtained *in vitro* through 3D printing or stereolithography is placed in a tissue defect, a photopolymerizable gel is additionally introduced into the defect, and polymerization is used to fix the scaffold in the tissue. A similar approach has been demonstrated in *ex vivo* repair of focal cartilage defects (with a diameter of 3 mm and a depth of ~ 2 mm) in pigs. At that, the construct obtained using a 3D printer was placed in the area of the cartilage defect, and a photo-composition was additionally introduced there: a mixture of eight-chain PEG-norbornene (with a molecular weight of 10 kDa) and PEG-dithiol (1 kDa) in the ratio of 1 : 1, as well as 0.05 wt.% of the photoinitiator Irgacure 2959. Then, polymerization was carried out for 8 min using a DLP printer (Autodesk Ember projection SLA-printer, $\lambda = 352$ nm, $I_{ex} = 5$ mW cm^{-2}).[212] Such a hybrid technology may be useful when translating classic scaffolds into the clinical medicine.

5.4. Drug delivery systems

3D printing is widely used to solve the problems of a personalized approach in medicine, in particular, to adapt pharmaceutical treatment, aimed at increasing its effectiveness, to each patient. Depending on the genetic predisposition, lifestyle, environmental conditions for each person, it is necessary to prepare personalized dosage forms. With this approach, 3D printing is a unique tool that allows one to quite easily create delivery matrices with an individual optimal dose and composition of drugs, as well as a personalized release profile.[213]

One of the first reports on the use of photopolymerizable hydrogels for drug delivery, in particular albumin, dates back to the early 1990s. Hubbel and co-workers[214] synthesized PEG block copolymers with oligo(D,L-lactic) acid or oligoglycolic acid containing end acrylate groups. Biodegradable hydrogels on their basis, obtained in the process of photoinduced crosslinking under the action of a UV lamp (BlakRay Model 3−100A, $\lambda = 365$ nm, $I_{ex} = 8$ mW cm^{-2}) in direct contact with tissues, demonstrated high adhesion to tissues and continuous effective release of albumin for 2 months. The choice of a suitable wavelength, power and dose of radiation eliminated the loss of protein stability and the biocompatibility decrease associated with the formation of radicals.[85, 215]

Due to their unique biological properties, hydrogels based on natural polysaccharides are of great interest as drug delivery matrices (see Section 3.1). For example, Zhang *et al.*[216] obtained biocompatible chitosan-based thermo- and pH-sensitive hydrogels for using them as carriers of antitumor and anti-inflammatory drugs. Under the action of a UV lamp (Osram Ultra-Vitalux 300-W), the authors formed *in situ* hydrogels from a graft copolymer of carboxymethylchitosan with *N*-isopropylacrylamide and glycidyl methacrylate in the presence of Irgacure 2959 initiator, which contained an anticancer drug (5-fluorouracil) and anti-inflammatory agent (diclofenac sodium). The release of these drugs was controlled by changing the degree of inoculation, pH and temperature of the medium, provid-

A.N.Generalova, P.A.Demina, R.A.Akasov, E.V.Khaydukov
Russ. Chem. Rev., 2023, **92** (2) RCR5068

21 of 26

ing drug protection at physiological temperature, low pH of the medium (*e.g.*, in a stomach) and demonstrating release under conditions with a higher pH (*e.g.*, in an intestine). Thus, the release of diclofenac sodium increased from 27% at pH 2.1 to 89% at pH 7.4

When delivering hydrophobic drugs, it is challenging to control the dose and duration of release. The introduction of such drugs into hydrophilic polymer matrices due to physical interactions does not guarantee their stable release over a long period of time. Cisneros *et al.*[217] demonstrated a delivery method for simvastatin, a hydrophobic drug that promotes bone growth and healing and prevents cartilage degradation by counteracting tumor necrosis factor, inhibiting bone morphogenetic protein, and improving osteogenic stimulation. Simvastatin was incorporated into polymeric micelles of triblock copolymers of polylactide and polyethylene glycol (PLA-PEG-PLA) and mixed with *N*-methacryloylchitosan and polyethylene glycol diacrylate (PEGDA); then, a crosslinking reaction under irradiation with a 405 nm LED (power of 48 W) in the presence of LAP was carried out. It was shown that the effect of the controlled release of simvastatin on osteogenic stimulation, as well as on the mechanical and biological properties of the hydrogel as an implant, depends significantly on the polymer compositions. Drug release continued for 17 weeks of follow-up, with cytocompatibility of hydrogels confirmed in all cases.

The creation of scaffolds that mimic the native extracellular matrix and are capable of releasing growth factors is one of the important tasks of tissue engineering. Modaresifar *et al.*[218] obtained a composite hydrogel based on methacrylated gelatin and chitosan nanoparticles containing angiogenic growth factor (bFGF) using photopolymerization under a UV lamp ($\lambda = 365$ nm, $I_{ex} = 10$ mW cm^{-2}). It was shown that this hydrogel promotes cell proliferation due to its biocompatible structure and provides a stable bFGF release profile, which is of great importance for angiogenesis processes.

The advantages of 3D printing technology, which allows adjustment of geometric dimensions of scaffolds and dosage of drugs, are reflected in the development of approaches to creation of constructs for specific patients. Such approaches are being used, for example, to create anatomically adaptable patches for personalized transdermal drug administration.[219] Goyanes *et al.*[220] used SLA printing to create a nose-shaped mask containing salicylic acid as a treatment for acne, an inflammatory skin disease. A commercial product, polycaprolactone with salicylic acid, was incorporated into a PEGDA–PEG–LAP photoinitiator composition that was cured by irradiation with a 405-nm laser. SLA printing demonstrated high resolution and achievement of the required drug loading without loss of drug activity, as well as the ability of construct fine-tuning in accordance with the anatomical features of the patient. These studies have shown the advantage of the SLA technology over traditional thermoplastic extrusion.[220]

One of the minimally invasive methods of drug delivery, which has been actively introduced into medical practice over the past 20 years, is based on the use of microneedles.[221, 222] Biosoluble microneedles started to be used in transdermal drug delivery to improve penetration of low and high molecular weight drugs through the skin barrier. Such instruments may be in the form of a lancet or a miniature hypodermic needle with a length of less than 500 μm, which can reduce injury and pain at the injection site. Hollow microneedles are capable of delivering drugs

both by diffusion and by the exit through the needle opening under the pressure, which allow adjustment of the release profile over an extended period of time. For example, Pere *et al.*[223] made polymer patches with microneedles in the form of pyramids or cones using 3D printing technology. These patches were produced using a Form 2 SLA printer (Formlabs) from a commercial Dental SG biocompatible polymer with inkjet printed insulin-xylitol coatings. A rapid release of insulin (~ 30 min) with maintaining the protein properties was demonstrated.

Caudill *et al.*[224] showed the capabilities of CLIP-technology (Carbon's S1 CLIP printer, $\lambda = 385$ nm, $I_{ex} = 1$ and 4 mW cm^{-2}) to create PEG-based microneedles, which were coated with model proteins (bovine serum albumin, ovalbumin and lysozyme) using the same technology. The high rate of *in vitro* and *in vivo* release, preservation of the enzyme activity, and maintenance of the release profile for 72 h indicate the promise of such a spatially controlled coating.

An innovative approach to microneedle fabrication using femtosecond laser two-photon polymerization (2PP) was presented by Ovsyanikov *et al.*[225] Three-dimensional microneedle devices with different aspect ratios were created from modified ceramic hybrid materials (Ormocer®) under the action of femtosecond laser pulses (duration of 60 fs, frequency of 94 MHz, $\lambda = 780$ nm, power of < 450 mW). It was found that microneedles do not break when penetrating into adipose tissue and the viability of human epidermal keratinocytes is preserved on their surface. These results demonstrate significant promise for the use of 2PP, which in turn allows the use of a variety of polymers, low-cost ceramics and other light-sensitive materials, as well as easy scale-up of the process for industrial application. In addition, the use of 2PP for microneedle fabrication is a fast and simple one-step process, which distinguishes it from traditional multi-step methods for making such specimen.

6. Conclusion

Based on photoinduced polymerization and crosslinking reactions, 3D printing methods such as SLA, DLP and CLIP allow quick and accurate fabrication of polymer structures of various architectures without the use of molds or mechanical processing. Significant progress in this area is associated with the development of flexible and adjustable radical photoprocesses that facilitate the development of approaches to the creation of special ink taking into account the features of photoprinting. However, despite the active exploitation of photopolymerization and crosslinking reactions, there remain the problems that limit the further progressive development of 3D printing.

First of all, it is necessary to increase the variety of ink with specific biological, rheological, physicochemical and mechanical properties. This direction includes the search for new precursors and photoinitiators, optimization and study of new conditions for conducting photoreactions, as well as the study of interaction between a photocomposition and cells. In addition, an important direction is the creation of ink capable of curing under longer wavelength irradiation, which provides mild conditions for radical photoreactions at a greater depth of light penetration.

Further development of approaches to perform photoinduced radical processes, such as orthogonal click reactions, redox and controlled processes, *in situ* crosslinking, *etc.*, will expand the range of methods for the formation of hydrogels from ink with low viscosity. This is an effective

tool for more efficient functioning and gradient inclusion of cells of various lines by changing scaffold rigidity. The absence of a high viscosity requirement also ensures the chemical variety of ink, including the possibility of creating multicomponent samples with controlled irradiation of a photocomposition by light. Moreover, in the future, it is necessary to study the mechanisms of reactions in more detail and develop methods for controlling ink photoreactions in order to obtain large centimeter-sized structurally organized constructs containing cells within a few seconds. Such advanced knowledge in the field of photoinduced reactions will determine the development of new 3D printing technologies, which promote creation of constructs with specific patient anatomy for clinical application.

One of the main problems of 3D printing of large TECs is the delivery of nutrients and the exchange of metabolites. Currently, to solve this complex problem, active research on photoreaction chemistry is being carried out to create prevascularized scaffolds that ensure the delivery of nutrients and the development of a blood circulatory system. This can be achieved through additional spatiotemporal control of reactions, as well as through the light-driven degradation of material throughout the construct volume. Controlling the ratio of growing and degrading blocks in a construct determines the architectonics of the channel system, in which vascular growth can occur.

At present, the concept of 4D printing, based on the study of material properties in time, is being actively developed; it is positioned as a method for studying fundamental biological problems. For example, this concept can be used to solve the important problem related to careful control and adjustment of tissue repair when using 3D tissue-engineered constructs, printed from compositions that meet biomedical requirements in terms of both material, functionality, and mechanical properties. In addition, TEC can act as a model for various diseases, which has great potential for studying the fundamental biological processes associated with the disease progression and finding new drugs for its treatment.

In conclusion, it is worth noting that further progress in tissue engineering is determined by the development of new approaches to light-driven production of multicomponent constructs containing cells and drugs, as well as large vascularized structures. In general, photoinduced 3D printing of TECs is developing at a very fast pace, and there are many challenges for further in-depth research of an interdisciplinary nature, which will open up new prospects in numerous biomedical applications of this technology.

7. List of abbreviations and designations

AFCT — Addition-Fragmentation Chain Transfer,
CAL — Computed Axial Lithography,
CLIP — Continuous Liquid Interface Production,
CRP — Controlled Radical Polymerization,
DLP — Digital Light Projection,
I_{ex} — excitation intensity,
FTI — Film Transfer Imaging,
GelMA — Methacrylated Gelatin,
GFP — Green Fluorescent Protein,
HA — Hyaluronic Acid,
n-HA — Nanohydroxyapatite,
LAP — Lithium Phenyl(2,4,6-Trimethylbenzoyl)Phosphinate,
LCD — Liquid Crystal Display,
MJP — Multi-Jet 3D Printing,
MSC — Mesenchymal Stem Cells,
2PP — Two-Photon Polymerization,
PCL — Polycaprolactone,
PE-1 — Tetrakis(3-Mercaptobutanoate) Pentaerythritol,
PEG — Polyethylene Glycol,
PEGDA — Polyethylene Glycol Diacrylate,
PETMP — Tetrakis(3-Mercaptopropionate) Pentaerythritol,
PLA — Polylactide,
PLGA — Copolymer of Lactide with Glycolide,
POSS — Silsesquioxan,
PμSL — Projection micro-Stereolithography,
PVA — Polyvinyl Alcohol,
QCS — Quaternized Chitosan,
RAFT — Reversible Addition-Fragmentation Transfer Polymerization,
RFP — Red Fluorescent Protein,
SLA — Stereolitography,
TEA — Triethanolamine,
TEC — Tissue-Engineering Constructs,
TMPMP — Tris(3-Mercaptopropionate) Trimethylolpropane,
TMI — Tris[2-(3-Mercaptopropionyloxy)Ethyl]Isocyanurate,
TTC — Sodium Trithiocarbonate,
TTT — Triallyl-1,3,5-Triazine-2,4,6(1H,3H,5H)-Trione,
VEGF — Vascular Endothelial Growth Factor,
UCNP — Upconversion Nanoparticles.

8. References

1. A.Khademhosseini, R.Langer, J.Borenstein, J.P.Vacanti. *Proc. Natl. Acad. Sci. USA*, **103**, 2480 (2006)
2. R.F.Pereira, P.J.Bártolo. *Engineering*, **1**, 090 (2015)
3. P.J.Bártolo, C.K.Chua, H.A.Almeida, S.M.Chou, A.S.C.Lim. *Virtual Phys. Prototyp.*, **4**, 203 (2009)
4. D.W.Hutmacher. *Biomaterials*, **21**, 2529 (2000)
5. X.Huang, X.Wang, Y.Zhao. *Dyes Pigm.*, **141**, 413 (2017)
6. J.L.Drury, D.J.Mooney. *Biomaterials*, **24**, 4337 (2003)
7. W.Tomal, J.Ortyl. *Polymers (Basel)*, **12**, 1073 (2020)
8. P.Bajaj, R.M.Schweller, A.Khademhosseini, J.L.West, R.Bashir. *Annu. Rev. Biomed. Eng.*, **16**, 247 (2014)
9. S.R.Caliari, J.A.Burdick. *Nat. Methods*, **13**, 405 (2016)
10. A.Gebhardt, J.-S.Hotter. *Additive Manufacturing: 3D Printing for Prototyping and Manufacturing.* (München: Hanser Publishers, 2016)
11. B.D.Fairbanks, M.P.Schwartz, C.N.Bowman, K.S.Anseth. *Biomaterials*, **30**, 6702 (2009)
12. K.S.Lim, J.H.Galarraga, X.Cui, G.C.J.Lindberg, J.A.Burdick, T.B.F.Woodfield. *Chem. Rev.*, **120**, 10662 (2020)
13. T.Woodfield, K.Lim, P.Morouco, R.Levato, J.Malda, F.Melchels. In *Reference Module in Materials Science and Materials Engineering*. (Ed. P.Ducheyne). (Oxford: Elsevier, 2017). P. 587

A.N.Generalova, P.A.Demina, R.A.Akasov, E.V.Khaydukov
Russ. Chem. Rev., 2023, **92** (2) RCR5068

23 of 26

14. A.I.Rudskoy, A.A.Popovich, A.F.Il'yushchenko, P.A.Vityaz', D.A.Kaledina. *Additivnye Tekhnologii. Materisly i tekhnologicheskie Protsessy. (Additive technologies. Materials and Technological Processes)* (St Petersburg: Politekh-Press, 2021)

15. A.Bagheri, J.Jin. *ACS Appl. Polym. Mater.*, **1**, 593 (2019)

16. H.Quan, T.Zhang, H.Xu, S.Luo, J.Nie, X.Zhu. *Bioact. Mater.*, **5**, 110 (2020)

17. S.Dadashi-Silab, S.Doran, Y.Yagci. *Chem. Rev.*, **116**, 10212 (2016)

18. C.S.O'Bryan, T.Bhattacharjee, S.Hart, C.P.Kabb, K.D.Schulze, I.Chilakala, B.S.Sumerlin, W.G.Sawyer, T.E.Angelini. *Sci. Adv.*, **3**, e1602800 (2017)

19. C.B.Highley, K.H.Song, A.C.Daly, J.A.Burdick. *Adv. Sci.*, **6**, 1801076 (2019)

20. J.Zhang, F.Dumur, P.Xiao, B.Graff, D.Bardelang, D.Gigmes, J.P.Fouassier, J.Lalevée. *Macromolecules*, **48**, 2054 (2015)

21. S.Beuermann, M.Buback, T.P.Davis, R.G.Gilbert, R.A.Hutchinson, O.F.Olaj, G.T.Russell, J.Schweer, A.M.van Herk. *Macromol. Chem. Phys.*, **198**, 1545 (1997)

22. S.C.Ligon, B.Husár, H.Wutzel, R.Holman, R.Liska. *Chem. Rev.*, **114**, 557 (2014)

23. K.S.Lim, B.S.Schon, N.V.Mekhileri, G.C.J.Brown, C.M.Chia, S.Prabakar, G.J.Hooper, T.B.F.Woodfield. *ACS Biomater. Sci. Eng.*, **2**, 1752 (2016)

24. M.J.Kade, D.J.Burke, C.J.Hawker. *J. Polym. Sci., Part A: Polym. Chem.*, **48**, 743 (2010)

25. S.C.Ligon-Auer, M.Schwentenwein, C.Gorsche, J.Stampfl, R.Liska. *Polym. Chem.*, **7**, 257 (2016)

26. Y.Jiang, J.Chen, C.Deng, E.J.Suuronen, Z.Zhong. *Biomaterials*, **35**, 4969 (2014)

27. C.E.Hoyle, C.N.Bowman. *Angew. Chem., Int. Ed.*, **49**, 1540 (2010)

28. A.B.Lowe. *Polym. Chem.*, **5**, 4820 (2014)

29. A.F.Senyurt, C.E.Hoyle, H.Wei, S.G.Piland, T.E.Gould. *Macromolecules*, **40**, 3174 (2007)

30. Appl. EP 1477511 A1 (2004)

31. P.Esfandiari, S.C.Ligon, J.J.Lagref, R.Frantz, Z.Cherkaoui, R.Liska. *J. Polym. Sci., Part A: Polym. Chem.*, **51**, 4261 (2013)

32. L.Chen, Q.Wu, G.Wei, R.Liu, Z.Li. *J. Mater. Chem. C*, **6**, 11561 (2018)

33. M.Abdallah, A.Hijazi, J.-T.Lin, B.Graff, F.Dumur, J.Lalevée. *ACS Appl. Polym. Mater.*, **2**, 2769 (2020)

34. A.G.Savelyev, K.N.Bardakova, E.V.Khaydukov, A.N.Generalova, V.K.Popov, B.N.Chichkov, V.A.Semchishen. *J. Photochem. Photobiol. A: Chem.*, **341**, 108 (2017)

35. J.D.Spikes, H.-R.Shen, P.Kopečková, J.Kopeček. *Photochem. Photobiol.*, **70**, 130 (1999)

36. K.L.Skubi, T.R.Blum, T.P.Yoon. *Chem. Rev.*, **116**, 10035 (2016)

37. R.J.DeRosa, M.C.Crutchley. *Coord. Chem. Rev.*, **233 – 234**, 351 (2002)

38. A.Allushi, C.Kutahya, C.Aydogan, J.Kreutzer, G.Yilmaz, Y.Yagci. *Polym. Chem.*, **8**, 1972 (2017)

39. K.Matyjaszewski, N.V.Tsarevsky. *J. Am. Chem. Soc.*, **136**, 6513 (2014)

40. X.Pan, M.Lamson, J.Yan, K.Matyjaszewski. *ACS Macro Lett.*, **4**, 192 (2015)

41. Y.Zhao, M.Yu, S.Zhang, Z.Wu, Y.Liu, C.-H.Peng, X.Fu. *Chem. Sci.*, **6**, 2979 (2015)

42. C.Gorsche, K.Seidler, P.Knaack, P.Dorfinger, T.Koch, J.Stampfl, N.Moszner, R.Liska. *Polym. Chem.*, **7**, 2009 (2016)

43. R.D.Goodridge, C.J.Tuck, R.J.M.Hague. *Prog. Mater. Sci.*, **57**, 229 (2012)

44. D.Zhou, R.P.Kuchel, P.B.Zetterlund. *Polym. Chem.*, **8**, 4177 (2017)

45. E.V.Chernikova, E.V.Sivtsov. *Polym. Sci., Ser. B*, **59**, 117 (2017)

46. H.Y.Park, C.J.Kloxin, A.S.Abuelyaman, J.D.Oxman, C.N.Bowman. *Macromolecules*, **45**, 5640 (2012)

47. M.Chen, M.J.MacLeod, J.A.Johnson. *ACS Macro Lett.*, **4**, 566 (2015)

48. M.Chen, Y.Gu, A.Singh, M.Zhong, A.M.Jordan, S.Biswas, L.T.J.Korley, A.C.Balazs, J.A.Johnson. *ACS Cent. Sci.*, **3**, 124 (2017)

49. W.L.Murphy, T.C.McDevitt, A.J.Engler. *Nat. Mater.*, **13**, 547 (2014)

50. S.Bertlein, G.Brown, K.S.Lim, T.Jungst, T.Boeck, T.Blunk, J.Tessmar, G.J.Hooper, T.B.F.Woodfield, J.Groll. *Adv. Mater.*, **29**, 1703404 (2017)

51. J.Van Hoorick, P.Gruber, M.Markovic, M.Rollot, G.-J.Graulus, M.Vagenende, M.Tromayer, J.Van Erps, H.Thienpont, J.C.Martins, S.Baudis, A.Ovsianikov, P.Dubruel, S.Van Vlierberghe. *Macromol. Rapid Commun.*, **39**, 1800181 (2018)

52. C.B.Highley, G.D.Prestwich, J.A.Burdick. *Curr. Opin. Biotechnol.*, **40**, 35 (2016)

53. X.Z.Shu, Y.Liu, F.Palumbo, G.D.Prestwich. *Biomaterials*, **24**, 3825 (2003)

54. X.Ma, X.Qu, W.Zhu, Y.-S.Li, S.Yuan, H.Zhang, J.Liu, P.Wang, C.S.E.Lai, F.Zanella, G.-S.Feng, F.Sheikh, S.Chien, S.Chen. *Proc. Natl. Acad. Sci. USA*, **113**, 2206 (2016)

55. A.V.Sochilina, A.G.Savelyev, R.A.Akasov, V.P.Zubov, E.V.Khaydukov, A.N.Generalova. *Russ. J. Bioorg. Chem.*, **47**, 828 (2021)

56. W.M.Gramlich, I.L.Kim, J.A.Burdick. *Biomaterials*, **34**, 9803 (2013)

57. S.L.Vega, M.Y.Kwon, K.H.Song, C.Wang, R.L.Mauck, L.Han, J.A.Burdick. *Nat. Commun.*, **9**, 614 (2018)

58. M.Y.Kwon, C.Wang, J.H.Galarraga, E.Puré, L.Han, J.A.Burdick. *Biomaterials*, **222**, 119451 (2019)

59. X.Zhang, P.Sun, L.Huangshan, B.-H.Hu, P.B.Messersmith. *Chem. Commun.*, **51**, 9662 (2015)

60. A.Abbadessa, M.M.Blokzijl, V.H.M.Mouser, P.Marica, J.Malda, W.E.Hennink, T.Vermonden. *Carbohydr. Polym.*, **149**, 163 (2016)

61. L.Pescosolido, W.Schuurman, J.Malda, P.Matricardi, F.Alhaique, T.Coviello, P.R.van Weeren, W.J.A.Dhert, W.E.Hennink, T.Vermonden. *Biomacromolecules*, **12**, 1831 (2011)

62. J.-H.Ahn, H.-S.Lee, J.-S.Lee, Y.-S.Lee, J.-L.Park, S.-Y.Kim, J.-A.Hwang, N.Kunkeaw, S.Y.Jung, T.J.Kim, K.-S.Lee, S.H.Jeon, I.Lee, B.H.Johnson, J.-H.Choi, Y.S.Lee. *Nat. Commun.*, **9**, 1166 (2018)

63. T.Cebe, N.Ahuja, F.Monte, K.Awad, K.Vyavhare, P.Aswath, J.Huang, M.Brotto, V.Varanasi. *J. Mater. Res.*, **35**, 58 (2020)

64. A.N.Generalova, V.V.Rocheva, A.V.Nechaev, D.A.Khochenkov, N.V.Sholina, V.A.Semchishen, V.P.Zubov, A.V.Koroleva, B.N.Chichkov, E.V.Khaydukov. *RSC Adv.*, **6**, 30089 (2016)

65. J.L Ifkovits, J.A.Burdick. *Tissue Eng.*, **13**, 2369 (2007)

66. Q.Li, J.Wang, S.Shahani, D.D.N.Sun, B.Sharma, J.H.Elisseeff, K.W.Leong. *Biomaterials*, **27**, 1027 (2006)

67. K.S.Lim, R.Levato, P.F.Costa, M.D.Castilho, C.R.Alcala-Orozco, K.M.A.van Dorenmalen, F.P.W.Melchels, D.Gawlitta, G.J.Hooper, J.Malda, T.B.F.Woodfield. *Biofabrication*, **10**, 034101 (2018)

68. K.S.Lim, M.H.Alves, L.A.Poole-Warren, P.J.Martens. *Biomaterials*, **34**, 7097 (2013)

69. J.-M.Lü, X.Wang, C.Marin-Muller, H.Wang, P.H.Lin, Q.Yao, C.Chen. *Expert Rev. Mol. Diagn.*, **9**, 325 (2009)

70. T.Serra, M.Ortiz-Hernandez, E.Engel, J.A.Planell, M.Navarro. *Mater. Sci. Eng. C*, **38**, 55 (2014)

71. S.A.Chesnokov, D.Y.Aleynik, R.S.Kovylin, V.V.Yudin, T.A.Egiazaryan, M.N.Egorikhina, M.I.Zaslavskaya, Y.P.Rubtsova, S.A.Gusev, S.G.Mlyavykh, I.L.Fedushkin. *Macromol. Biosci.*, **21**, 2000402 (2021)

72. T.M.Seck, F.P.W.Melchels, J.Feijen, D.W.Grijpma. *J. Control. Release*, **148**, 34 (2010)

73. B.Zhang, S.Li, H.Hingorani, A.Serjouei, L.Larush, A.A.Pawar, W.H.Goh, A.H.Sakhaei, M.Hashimoto, K.Kowsari, S.Magdassi, Q.Ge. *J. Mater. Chem. B*, **6**, 3246 (2018)

74. J.Palaganas, A.C.de Leon, J.Mangadlao, N.Palaganas, A.Mael, Y.J.Lee, H.Y.Lai, R.Advincula. *Macromol. Mater. Eng.*, **302**, 1600477 (2017)

75. D.L.Hern, J.A.Hubbell. *J. Biomed. Mater. Res.*, **39**, 266 (1998)

76. A.Eibel, D.E.Fast, G.Gescheidt. *Polym. Chem.*, **9**, 5107 (2018)

77. K.S.Lim, B.J.Klotz, G.C.J.Lindberg, F.P.W.Melchels, G.J.Hooper, J.Malda, D.Gawlitta, T.B.F.Woodfield. *Macromol. Biosci.*, **19**, 1900098 (2019)

78. J.Lalevée, M.-A.Tehfe, F.Dumur, D.Gigmes, B.Graff, F.Morlet-Savary, J.-P.Fouassier. *Macromol. Rapid Commun.*, **34**, 239 (2013)

79. K.Kaastrup, H.D.Sikes. *Chem. Soc. Rev.*, **45**, 532 (2016)

80. Patent US 4575330 (1986)

81. Z.Ma, X.Niu, Z.Xu, J.Guo. *J. Appl. Polym. Sci.*, **131**, 40352 (2014)

82. P.Demina, N.Arkharova, I.Asharchuk, K.Khaydukov, D.Karimov, V.Rocheva, A.Nechaev, Y.Grigoriev, A.Generalova, E.Khaydukov. *Molecules*, **24**, 2476 (2019)

83. A.Ovsianikov, S.Schlie, A.Ngezahayo, A.Haverich, B.N.Chichkov. *J. Tissue Eng. Regen. Med.*, **1**, 443 (2007)

84. H.K.Park, M.Shin, B.Kim, J.W.Park, H.Lee. *NPG Asia Mater.*, **10**, 82 (2018)

85. S.J.Bryant, C.R.Nuttelman, K.S.Anseth. *J. Biomater. Sci., Polym. Ed.*, **11**, 439 (2000)

86. V.Srivastava, P.P.Singh. *RSC Adv.*, **7**, 31377 (2017)

87. M.V.Encinas, A.M.Rufs, S.Bertolotti, C.M.Previtali. *Macromolecules*, **34**, 2845 (2001)

88. S.Kim, C.-C.Chu. *Fibers Polym.*, **10**, 14 (2009)

89. A.Bagheri, J.Yeow, H.Arandiyan, J.Xu, C.Boyer, M.Lim. *Macromol. Rapid Commun.*, **37**, 905 (2016)

90. X.Wan, Y.Zhao, J.Xue, F.Wu, X.Fang. *J. Photochem. Photobiol. A: Chem.*, **202**, 74 (2009)

91. Q.Liang, L.Zhang, Y.Xiong, Q.Wu, H.Tang. *J. Photochem. Photobiol. A: Chem.*, **299**, 9 (2015)

92. D.J.Lougnot, J.P.Fouassier. *J. Polym. Sci., Part A: Polym. Chem.*, **26**, 1021 (1988)

93. A.D.Rouillard, C.M.Berglund, J.Y.Lee, W.J.Polacheck, Y.Tsui, L.J.Bonassar, B.J.Kirby. *Tissue Eng., Part C*, **17**, 173 (2011)

94. M.Liu, M.-D.Li, J.Xue, D.L.Phillips. *J. Phys. Chem. A*, **118**, 8701 (2014)

95. E.Andrzejewska. *Prog. Polym. Sci.*, **26**, 605 (2001)

96. G.Ullrich, B.Ganster, U.Salz, N.Moszner, R.Liska. *J. Polym. Sci., Part A: Polym. Chem.*, **44**, 1686 (2006)

97. W.Majima, T.Schnabel, W.Weber. *Makromol. Chem.*, **192**, 2307 (1991)

98. S.F.Yates, G.B.Schuster. *J. Org. Chem.*, **49**, 3349 (1984)

99. J.Lalevée, F.Morlet-Savary, M.El Roz, X.Allonas, J.P.Fouassier. *Macromol. Chem. Phys.*, **210**, 311 (2009)

100. J.Lalevée, F.Morlet-Savary, M.A.Tehfe, B.Graff, J.P.Fouassier. *Macromolecules*, **45**, 5032 (2012)

101. *Dyes and Chromophors in Polymer Science*. (Eds J.Lalevée, J.-P.Fouassier). Wiley, Hoboken, NJ, 2015

102. J.Malda, J.Visser, F.P.Melchels, T.Jüngst, W.E.Hennink, W.J.A.Dhert, J.Groll, D.W.Hutmacher. *Adv. Mater.*, **25**, 5011 (2013)

103. S.G.Bertolotti, C.M.Previtali, A.M.Rufs, M.V.Encinas. *Macromolecules*, **32**, 2920 (1999)

104. D.A.Fancy, T.Kodadek. *Proc. Natl. Acad. Sci. USA*, **96**, 6020 (1999)

105. D.Kim, J.W. Stansbury. *J. Polym. Sci., Part A: Polym. Chem.*, **47**, 3131 (2009)

106. A.K.Nguyen, R.J.Narayan. *Mater. Today*, **20**, 314 (2017)

107. E.V.Khaidukov. Doctoral Thesis in Physical and Mathematical Sciences, FNITS, 'Crystallography and Photonics', 2021

108. S.Maruo, O.Nakamura, S.Kawata. *Opt. Lett.*, **22**, 132 (1997)

109. T.Weib, G.Hildebrand, R.Schade, K.Liefeith. *Eng. Life Sci.*, **9**, 384 (2009)

110. B.A.Reinhardt, L.L.Brott, S.J.Clarson, A.G.Dillard, J.C.Bhatt, R.Kannan, L.Yuan, G.S.He, P.N.Prasad. *Chem. Mater.*, **10**, 1863 (1998)

111. K.J.Schafer, J.M.Hales, M.Balu, K.D.Belfield, E.W.Van Stryland, D.J.Hagan. *J. Photochem. Photobiol. A: Chem.*, **162**, 497 (2004)

112. A.Doraiswamy, C.Jin, R.Narayan, P.Mageswaran, P.Mente, R.Modi, R.Auyeung, D.Chrisey, A.Ovsianikov, B.Chichkov. *Acta Biomater.*, **2**, 267 (2006)

113. H.Y.Woo, B.Liu, B.Kohler, D.Korystov, A.Mikhailovsky, G.C.Bazan. *J. Am. Chem. Soc.*, **127**, 14721 (2005)

114. Y.E.Begantsova, R.Zvagelsky, E.V.Baranov, D.A.Chubich, Y.V.Chechet, D.A.Kolymagin, A.V.Pisarenko, A.G.Vitukhnovsky, S.A.Chesnokov. *Eur. Polym. J.*, **145**, 110209 (2021)

115. A.N.Generalova, B.N.Chichkov, E.V.Khaydukov. *Adv. Colloid Interface Sci.*, **245**, 1 (2017)

116. J.Méndez-Ramos, J.C.Ruiz-Morales, P.Acosta-Mora, N.M.Khaidukov. *J. Mater. Chem. C*, **4**, 801 (2016)

117. V.V.Rocheva, A.V.Koroleva, A.G.Savelyev, K.V.Khaydukov, A.N.Generalova, A.V.Nechaev, A.E.Guller, V.A.Semchishen, B.N.Chichkov, E.V.Khaydukov. *Sci. Rep.*, **8**, 3663 (2018)

118. T.Jungst, W.Smolan, K.Schacht, T.Scheibel, J.Groll. *Chem. Rev.*, **116**, 1496 (2016)

119. E.G.Gordeev, V.P.Ananikov. *Russ. Chem. Rev.*, **89**, 1507 (2020)

120. S.You, J.Li, W.Zhu, C.Yu, D.Mei, S.Chen. *J. Mater. Chem. B*, **6**, 2187 (2018)

121. D.Choudhury, S.Anand, M.W.Naing. *Int. J. Bioprint.*, **4**, (2018)

122. Y.S Zhang, G.Haghiashtiani, T.Hübscher, D.J.Kelly, J.M.Lee, M.Lutolf, M.C.McAlpine, W.Y.Yeong, M.Zenobi-Wong, J.Malda. *Nat. Rev. Methods Prim.*, **1**, 75 (2021)

123. S.Kyle, Z.M Jessop, A.Al-Sabah, I.S.Whitaker. *Adv. Health. Mater.*, **6**, 1700264 (2017)

124. J.E.Trachtenberg, J.K.Placone, B.T.Smith, C.M.Piard, M.Santoro, D.W.Scott, J.P.Fisher, A.G.Mikos. *ACS Biomater. Sci. Eng.*, **2**, 1771 (2016)

125. A.Skardal, J.Zhang, L.McCoard, X.Xu, S.Oottamasathien, G.D.Prestwich. *Tissue Eng., Part A*, **16**, 2675 (2010)

126. L.A.Hockaday, K.H.Kang, N.W.Colangelo, P.Y.C.Cheung, B.Duan, E.Malone, J.Wu, L.N.Girardi, L.J.Bonassar, H.Lipson, C.C.Chu, J.T.Butcher. *Biofabrication*, **4**, 035005 (2012)

127. A.C.Daly, L.Riley, T.Segura, J.A.Burdick. *Nat. Rev. Mater.*, **5**, 20 (2020)

128. L.Ouyang, C.B.Highley, W.Sun, J.A.Burdick. *Adv. Mater.*, **29**, 1604983 (2017)

129. J.H.Galarraga, M.Y.Kwon, J.A.Burdick. *Sci. Rep.*, **9**, 19987 (2019)

130. D.Godec, B.Šantek, R.Ludwig, M.Andlar, I.Reziá, F.Ivušić, A.Pilipović, D.Oros, T.Reziá, M.Šercer. *Food Technol. Biotechnol.*, **57**, 272 (2019)

131. S.Tibbits. *Archit. Des.*, **84**, 116 (2014)

132. X.Kuang, D.J.Roach, J.Wu, C.M.Hamel, Z.Ding, T.Wang, M.L.Dunn, H.J.Qi. *Adv. Funct. Mater.*, **29**, 1805290 (2019)

133. S.Zeng, Y.Gao, Y.Feng, H.Zheng, H.Qiu, J.Tan. *Smart Mater. Struct.*, **28**, 105031 (2019)

134. Z.Ding, O.Weeger, H.J.Qi, M.L.Dunn. *Mater. Des.*, **137**, 256 (2018)

135. Y.Mao, Z.Ding, C.Yuan, S.Ai, M.Isakov, J.Wu, T.Wang, M.L.Dunn, H.J.Qi. *Sci. Rep.*, **6**, 24761 (2016)

136. F.Momeni, N.S.M.M.Hassani, X.Liu, J.Ni. *Mater. Des.*, **122**, 42 (2017)

A.N.Generalova, P.A.Demina, R.A.Akasov, E.V.Khaydukov
Russ. Chem. Rev., 2023, **92** (2) RCR5068

25 of 26

137. H.-W.Kang, S.J.Lee, I.K.Ko, C.Kengla, J.J.Yoo, A.Atala. *Nat. Biotechnol.*, **34**, 312 (2016)
138. B.Zhang, R.Cristescu, D.B.Chrisey, R.J.Narayan. *Int. J. Bioprint.*, **6**, 19 (2020)
139. S.Boularaoui, G.Al Hussein, K.A.Khan, N.Christoforou, C.Stefanini. *Bioprinting*, **20**, e00093 (2020)
140. J.Xiao, G.Ji, Y.Zhang, G.Ma, V.Mechtcherine, J.Pan, L.Wang, T.Ding, Z.Duan, S.Du. *Cem. Concr. Compos.*, **122**, 104115 (2021)
141. R.Chang, J.Nam, W.Sun. *Tissue Eng., Part A*, **14**, 41 (2008)
142. B.Byambaa, N.Annabi, K.Yue, G.Trujillo-de Santiago, M.M.Alvarez, W.Jia, M.Kazemzadeh-Narbat, S.R.Shin, A.Tamayol, A Khademhosseini. *Adv. Health. Mater.*, **6**, 1700015 (2017)
143. V.H.M.Mouser, R.Levato, L.J.Bonassar, D.D.D'Lima, D.A.Grande, T.J.Klein, D.B.F.Saris, M.Zenobi-Wong, D.Gawlitta, J.Malda. *Cartilage*, **8**, 327 (2017)
144. B.Duan. *Ann. Biomed. Eng.*, **45**, 195 (2017)
145. F.-Y.Hsieh, S.Hsu. *Organogenesis*, **11**, 153 (2015)
146. Patent US 638905 (1986)
147. J.Wang, A.Goyanes, S.Gaisford, A.W.Basit. *Int. J. Pharm.*, **503**, 207 (2016)
148. J.Huang, Q.Qin, J.Wang. *Processes*, **8**, 1138 (2020)
149. R.Levato, K.S.Lim, W.Li, A.U.Asua, L.B.Peña, M.Wang, M.Falandt, P.N.Bernal, D.Gawlitta, Y.S.Zhang, T.B.F.Woodfield, J.Malda. *Mater. Today Bio*, **12**, 100162 (2021)
150. J.Z.Manapat, Q.Chen, P.Ye, R.C.Advincula. *Macromol. Mater. Eng.*, **302**, 1600553 (2017)
151. X.Wang, M.Jiang, Z.Zhou, J.Gou, D.Hui. *Composites, Part B*, **110**, 442 (2017)
152. Y.-L.Cheng, F.Chen. *Mater. Sci. Eng. C*, **81**, 66 (2017)
153. C.Sun, N.Fang, D.M.Wu, X.Zhang. *Sens. Actuators, A*, **121**, 113 (2005)
154. K.M.Arif, T.Murakami. *Int. J. Adv. Manuf. Technol.*, **41**, 527 (2009)
155. B.E.Kelly, I.Bhattacharya, H.Heidari, M.Shusteff, C.M.Spadaccini, H.K.Taylor. *Science*, **363**, 1075 (2019)
156. J.R.Tumbleston, D.Shirvanyants, N.Ermoshkin, R.Janusziewicz, A.R.Johnson, D.Kelly, K.Chen, R.Pinschmidt, J.P.Rolland, A.Ermoshkin, E.T.Samulski, J.M.DeSimone. *Science*, **347**, 1349 (2015)
157. J.H.Moon, S.Yang. *J. Macromol. Sci., Part C: Polym. Rev.*, **45**, 351 (2005)
158. A.M.Prenen, J.C.A.H.van der Werf, C.W.M.Bastiaansen, D.J.Broer. *Adv. Mater.*, **21**, 1751 (2009)
159. J.Torgersen, X.-H.Qin, Z.Li, A.Ovsianikov, R.Liska, J.Stampfl. *Adv. Funct. Mater.*, **23**, 4542 (2013)
160. W.R.Zipfel, R.M.Williams, W.W.Webb. *Nat. Biotechnol.*, **21**, 1369 (2003)
161. A.Ovsianikov. *Investigation of Two-photon Polymerization Technique for Applications in Photonics and Biomedicine.* (Hannover: Cuvillier Verlag, 2009)
162. K.Obata, A.El-Tamer, L.Koch, U.Hinze, B.N.Chichkov. *Light Sci. Appl.*, **2**, e116 (2013)
163. R.Liang, Y.Gu, Y.Wu, V.Bunpetch, S.Zhang. *ACS Biomater. Sci. Eng.*, **7**, 806 (2021)
164. B.Grigoryan, D.W.Sazer, A.Avila, J.L.Albritton, A.Padhye, A.H.Ta, P.T.Greenfield, D.L.Gibbons, J.S.Miller. *Sci. Rep.*, **11**, 3171 (2021)
165. V.Gupta, B.Paull, P.Nesterenko. *3D Printing in Chemical Sciences: Applications Across Chemistry*. (Cambridge: RSC Publising, 2019)
166. S.Pahoff, C.Meinert, O.Bas, L.Nguyen, T.J.Klein, D.W.Hutmacher. *J. Mater. Chem. B*, **7**, 1761 (2019)
167. J.H.Correia, J.A.Rodrigues, S.Pimenta, T.Dong, Z.Yang. *Pharmaceutics*, **13**, 1332 (2021)
168. A.Sabnis, M.Rahimi, C.Chapman, K.T.Nguyen. *J. Biomed. Mater. Res., Part A*, **91**, 52 (2009)
169. S.Buonvino, M.Ciocci, D.Seliktar, S.Melino. *Int. J. Mol. Sci.*, **22**, 6095 (2021)
170. P.E.Donnelly, T.Chen, A.Finch, C.Brial, S.A.Maher, P.A.Torzilli. *J. Biomater. Sci., Polym. Ed.*, **28**, 582 (2017)
171. Z.Wang, X.Jin, R.Dai, J.F.Holzman, K.Kim. *RSC Adv.*, **6**, 21099 (2016)
172. D.Petta, D.W.Grijpma, M.Alini, D.Eglin, M.D'Este. *ACS Biomater. Sci. Eng.*, **4**, 3088 (2018)
173. A.G.Savelyev, A.V.Sochilina, R.A.Akasov, A.V.Mironov, A.Y.Kapitannikova, T.N.Borodina, N.V.Sholina, K.V.Khaydukov, A.V.Zvyagin, A.N.Generalova, E.V.Khaydukov. *Front. Bioeng. Biotechnol.*, **9**, (2021)
174. S.Chu, M.M.Maples, S.J.Bryant. *Acta Biomater.*, **109**, 37 (2020)
175. P.Yang, C Li, M.Lee, A.Marzvanyan, Z.Zhao, K.Ting, C.Soo, Z.Zheng. *Tissue Eng., Part A*, **26**, 1112 (2020)
176. Z.Wang, R.Abdulla, B.Parker, R.Samanipour, S.Ghosh, K.Kim. *Biofabrication*, **7**, 045009 (2015)
177. K.Gwon, E.Kim, G.Tae. *Acta Biomater.*, **49**, 284 (2017)
178. Z.Wang, H.Kumar, Z.Tian, X.Jin, J.F.Holzman, F.Menard, K.Kim. *ACS Appl. Mater. Interfaces*, **10**, 26859 (2018)
179. A.Ovsianikov, S.Mühleder, J.Torgersen, Z.Li, X.-H.Qin, S.Van Vlierberghe, P.Dubruel, W.Holnthoner, H.Redl, R.Liska, J.Stampfl. *Langmuir*, **30**, 3787 (2014)
180. Y.Chen, J.Zhang, X.Liu, S.Wang, J.Tao, Y.Huang, W.Wu, Y.Li, K.Zhou, X.Wei, S.Chen, X.Li, X.Xu, L.Cardon, Z.Qian, M.Gou. *Sci. Adv.*, **6**, eaba7406 (2020)
181. A.C.P.de Vasconcelos, R.P.Morais, G.B.Novais, S.da S.Barroso, L.R.O.Menezes, S.dos Santos, L.P.da Costa, C.B.Correa, P.Severino, M.Z.Gomes, R.L.C.Albuquerque Jr., J.C.Cardoso. *Nanomed. Nanotechnol., Biol. Med.*, **29**, 102272 (2020)
182. X.Zhang, Y.He, P.Huang, G.Jiang, M.Zhang, F.Yu, W.Zhang, G.Fu, Y.Wang, W.Li, H.Zeng. *Composites, Part B*, **197**, 108183 (2020)
183. Y.Wang, X.Lan, S.Zuo, Y.Zou, S.Li, Z.Tang, Y.Wang. *RSC Adv.*, **11**, 20997 (2021)
184. Y.Huo, Y.Xu, X.Wu, E.Gao, A.Zhan, Y.Chen, Y.Zhang, Y.Hua, W.Swieszkowski, Y.S.Zhang, G.Zhou. *Adv. Sci.*, **9**, 2202181 (2022)
185. P.Chen, L.Ning, P.Qiu, J.Mo, S.Mei, C.Xia, J.Zhang, X.Lin, S.Fan. *J. Tissue Eng. Regen. Med.*, **13**, 682 (2019)
186. S.A.Schoonraad, K.M.Fischenich, K.N.Eckstein, V.Crespo-Cuevas, L.M.Savard, A.Muralidharan, A.A.Tomaschke, A.C.Uzcategui, M.A.Randolph, R.R.McLeod, V.L.Ferguson, S.J.Bryant. *Biofabrication*, **13**, 044106 (2021)
187. Y.Ding, R.Fu, C.P.Collins, S.Yoda, C.Sun, G.A.Ameer. *Adv. Health. Mater.*, **11**, 2201955 (2022)
188. D.Kalhori, N.Zakeri, M.Zafar-Jafarzadeh, L.Moroni, M.Solati-Hashjin. *Bioprinting*, **28**, e00221 (2022)
189. P.Kerscher, J.A.Kaczmarek, S.E.Head, M.E.Ellis, W.J.Seeto, J.Kim, S.Bhattacharya, V.Suppiramaniam, E.A.Lipke. *ACS Biomater. Sci. Eng.*, **3**, 1499 (2017)
190. D.V.Deshmukh, P.Reichert, J.Zvick, C.Labouesse, V.Künzli, O.Dudaryeva, O.Bar-Nur, M.W.Tibbitt, J.Dual. *Adv. Funct. Mater.*, **32**, 2113038 (2022)
191. S.O.L.de Souza, S.M.de Oliveira, L.M.Silva, R.L.Oréfice. *J. Appl. Polym. Sci.*, **139**, (2022)
192. W.Kiratitanaporn, D.B.Berry, A.Mudla, T.Fried, A.Lao, C.Yu, N.Hao, S.R.Ward, S.Chen. *Biomater. Adv.*, **142**, 213171 (2022)
193. H.Li, K.Yu, P.Zhang, Y.Ye, Q.Shu. *J. Biomater. Appl.*, **37**, 538 (2022)
194. P.Wang, Y.Sun, X.Shi, H.Shen, H.Ning, H.Liu. *Bio-Design Manuf.*, **4**, 344 (2021)
195. S.Krishnamoorthy, S.Wadnap, B.Noorani, H.Xu, C.Xu. *Eur. Polym. J.*, **124**, 109487 (2020)
196. J.R.Thompson, K.S.Worthington, B.J.Green, N.K.Mullin, C.Jiao, E.E.Kaalberg, L.A.Wiley, I.C.Han, S.R.Russell, E.H.Sohn, C.A.Guymon, R.F.Mullins, E.M.Stone, B.A.Tucker. *Acta Biomater.*, **94**, 204 (2019)

197. N.Monteiro, G.Thrivikraman, A.Athirasala, A.Tahayeri, C.M.França, J.L.Ferracane, L.E.Bertassoni. *Dent. Mater.*, **34**, 389 (2018)

198. A.MacAdam, E.Chaudry, C.D.McTiernan, D.Cortes, E.J.Suuronen, E.I.Alarcon. *Front. Bioeng. Biotechnol.*, **10**, (2022)

199. C.Pascual-Garrido, E.A.Aisenbrey, F.Rodriguez-Fontan, K.A.Payne, S.J.Bryant, L.R.Goodrich. *Am. J. Sports Med.*, **47**, 212 (2019)

200. Y.Zhang, Y.Zheng, F.Shu, R.Zhou, B.Bao, S.Xiao, K.Li, Q.Lin, L.Zhu, Z.Xia. *Carbohydr. Polym.*, **276**, 118752 (2022)

201. N.Vaudreuil, K.Henrikson, P.Pohl, A.Lee, H.Lin, A.Olsen, Q.Dong, M.Dombrowski, J.Kang, N.Vo, J.Lee, G.Sowa. *J. Orthop. Res.*, **37**, 1451 (2019)

202. V.Keriquel, F Guillemot, I.Arnault, B.Guillotin, S.Miraux, J.Amédée, J.-C.Fricain, S.Catros. *Biofabrication*, **2**, 014101 (2010)

203. D.Hakobyan, O.Kerouredan, M.Remy, N.Dusserre, C.Medina, R.Devillard, J.-C.Fricain, H.Oliveira. In *3D Bioprinting*. *(Ser. Methods in Molecular Biology*. Vol. 2140). (Ed. J.M.Crook). (New York: Humana, 2020). P. 135

204. O.Kérourédan, D.Hakobyan, M.Rémy, S.Ziane, N.Dusserre, J.-C.Fricain, S.Delmond, N.B.Thébaud, R.Devillard. *Biofabrication*, **11**, 045002 (2019)

205. P.Karami, V.K.Rana, Q.Zhang, A.Boniface, Y.Guo, C.Moser, D.P.Pioletti. *Biomacromolecules*, **23**, 5007 (2022)

206. A.Urciuolo, I.Poli, L.Brandolino, P.Raffa, V.Scattolini, C.Laterza, G.G.Giobbe, E.Zambaiti, G.Selmin, M.Magnussen, L.Brigo, P.De Coppi, S.Salmaso, M.Giomo, N.Elvassore. *Nat. Biomed. Eng.*, **4**, 901 (2020)

207. C.Di Bella, S.Duchi, C.D.O'Connell, R.Blanchard, C.Augustine, Z.Yue, F.Thompson, C.Richards, S.Beirne, C.Onofrillo, S.H.Bauquier, S.D.Ryan, P.Pivonka, G.G.Wallace, P.F.Choong. *J. Tissue Eng. Regen. Med.*, **12**, 611 (2018)

208. G.Ying, J.Manríquez, D.Wu, J.Zhang, N.Jiang, S.Maharjan, D.H.Hernández Medina, Y.S.Zhang. *Mater. Today Bio*, **8**, 100074 (2020)

209. K.Ma, T.Zhao, L.Yang, P.Wang, J.Jin, H.Teng, D.Xia, L.Zhu, L.Li, Q Jiang, X.Wang. *J. Adv. Res.*, **23**, 123 (2020)

210. J.P.Quint, A.Mostafavi, Y.Endo, A.Panayi, C.S.Russell, A.Nourmahnad, C.Wiseman, L.Abbasi, M.Samandari, A.Sheikhi, K.Nuutila, I.Sinha, A.Tamayol. *Adv. Health. Mater.*, **10**, 2002152 (2021)

211. M.Xie, Y.Shi, C.Zhang, M.Ge, J.Zhang, Z.Chen, J.Fu, Z.Xie, Y.He. *Nat. Commun.*, **13**, 3597 (2022)

212. E.A.Aisenbrey, A.Tomaschke, E.Kleinjan, A.Muralidharan, C.Pascual-Garrido, R.R.McLeod, V.L.Ferguson, S.J.Bryant. *Macromol. Biosci.*, **18**, 1700267 (2018)

213. A.Zamboulis, G.Michailidou, I.Koumentakou, D.N.Bikiaris. *Pharmaceutics*, **14**, 145 (2022)

214. A.S.Sawhney, C.P.Pathak, J.A.Hubbell. *Macromolecules*, **26**, 581 (1993)

215. L.Pescosolido, S.Miatto, C.Di Meo, C.Cencetti, T.Coviello, F.Alhaique, P.Matricardi. *Eur. Biophys. J.*, **39**, 903 (2010)

216. L.Zhang, L.Wang, B.Guo, P.X.Ma. *Carbohydr. Polym.*, **103**, 110 (2014)

217. K.Cisneros, N.Chowdhury, E.Coleman, T.Ferdous, H.Su, J.A.Jennings, J.D.Bumgardner, T.Fujiwara. *Macromol. Biosci.*, **21**, 2100123 (2021)

218. K.Modaresifar, A.Hadjizadeh, H.Niknejad. *Artif. Cells Nanomed. Biotechnol.*, **46**, 1799 (2018)

219. C.I.Gioumouxouzis, C.Karavasili, D.G.Fatouros. *Drug Discov. Today*, **24**, 636 (2019)

220. A.Goyanes, U.Det-Amornrat, J.Wang, A.W.Basit, S.Gaisford. *J. Control. Release*, **234**, 41 (2016)

221. A.Alkilani, M.T.McCrudden, R.Donnelly. *Pharmaceutics*, **7**, 438 (2015)

222. M.R.Prausnitz, S.Mitragotri, R.Langer. *Nat. Rev. Drug Discov.*, **3**, 115 (2004)

223. C.P.P.Pere, S.N.Economidou, G.Lall, C.Ziraud, J.S.Boateng, B.D.Alexander, D.A.Lamprou, D.Douroumis. *Int. J. Pharm.*, **544**, 425 (2018)

224. C.L.Caudill, J.L.Perry, S.Tian, J.C.Luft, J.M.DeSimone. *J. Control. Release*, **284**, 122 (2018)

225. A.Ovsianikov, B.Chichkov, P.Mente, N.A.Monteiro-Riviere, A.Doraiswamy, R.J.Narayan. *Int. J. Appl. Ceram. Technol.*, **4**, 22 (2007)